

Invited review article

# The causes of continental arc flare ups and drivers of episodic magmatic activity in Cordilleran orogenic systems

James B. Chapman<sup>a,\*</sup>, Jessie E. Shields<sup>a</sup>, Mihai N. Ducea<sup>b,c</sup>, Scott R. Paterson<sup>d</sup>, Snir Attia<sup>e</sup>, Katie E. Ardill<sup>f</sup>

<sup>a</sup> Department of Geology and Geophysics, University of Wyoming, Laramie, WY 82071, USA

<sup>b</sup> Department of Geosciences, University of Arizona, Tucson, AZ 85721, USA

<sup>c</sup> Faculty of Geology and Geophysics, University of Bucharest, Bucharest, Romania

<sup>d</sup> Department of Earth Sciences, University of Southern California, Los Angeles, CA 90089, USA

<sup>e</sup> New Mexico Bureau of Geology and Mineral Resources, New Mexico Institute of Mining and Technology, Socorro, NM 87801, USA

<sup>f</sup> Department of Geology, California State University, Sacramento, CA 95819, USA

## ABSTRACT

Continental arcs in Cordilleran orogenic systems display episodic changes in magma production rate, alternating between flare ups ( $70\text{--}90\text{ km}^3\text{ km}^{-1}\text{ Myr}^{-1}$ ) and lulls ( $< 20\text{ km}^3\text{ km}^{-1}\text{ Myr}^{-1}$ ) on timescales of tens of millions of years. Arc segments or individual magmatic suites may have even higher rates, up several  $100\text{ s of km}^3\text{ km}^{-1}\text{ Myr}^{-1}$ , during flare ups. These rates are largely determined by estimating volumes of arc crust, but do not reflect melt production from the mantle. The bulk of mantle-derived magmas are recycled back into the mantle by delamination of arc roots after differentiation in the deep crust. Mantle-derived melt production rates for continental arcs are estimated to be  $140\text{--}215\text{ km}^3\text{ km}^{-1}\text{ Myr}^{-1}$  during flare ups and  $\leq 15\text{ km}^3\text{ km}^{-1}\text{ Myr}^{-1}$  during lulls. Melt production rates averaged over multiple magmatic cycles are consistent with independent estimates for partial melting of the mantle wedge in subduction zones, however, the rates during flare ups and lulls are both anomalously high and anomalously low, respectively. The difference in mantle-derived melt production between flare ups and lulls is larger than predicted by petrologic and numerical models that explore the range of globally observed subduction parameters (e.g., convergence rate, height of the mantle wedge). This suggests that other processes are required to increase magmatism during flare ups and suppress magmatism during lulls. There are many viable explanations, but one possibility is that crystallized melts from the asthenospheric mantle wedge are temporarily stored in the deep lithosphere during lulls and then remobilized during flare ups. Basaltic melts may stall in the mantle lithosphere in inactive parts of the arc system, like the back-arc, refertilizing the mantle lithosphere and suppressing melt delivery to the lower crust. Subsequent landward arc migration (i.e., toward the interior of the continent) may encounter such refertilized mantle lithosphere magma source regions, contributing to magmatic activity during a flare up. A review of continental arcs globally suggests that flare ups commonly coincide with landward arc migration and that this migration may start tens of millions of years before the flare up occurs. The region of magmatic activity, or arc width, can also expand significantly during a flare up. Arc migration or expansion into different mantle source regions and across lithospheric and crustal boundaries can cause temporal shifts in the radiogenic isotopic composition of magmatism. In the absence of arc migration, temporal shifts are more muted. Isotopic studies of mantle xenoliths and exposures of deep arc crust suggest that that primary, mantle-derived magmas generated during flare ups reflect substantial contributions from the subcontinental mantle lithosphere. Arc migration may be caused by a variety of mechanisms, including slab anchoring or slab folding in the mantle transition zone that could generate changes in slab dip. Episodic slab shallowing is associated with many tectonic processes in Cordilleran orogenic systems, like alternations between shortening and extension in the upper plate. Studies of arc migration may help to link irregular magmatic production in continental arcs with geodynamic models for orogenic cyclicity.

## 1. Introduction

Despite up to hundreds of millions of years of relatively stable plate margin configurations (e.g., North and South American Cordillera), magma production in continental arcs is highly episodic with repeated intervals of increased magma production, called flare ups, alternating with intervals of decreased magma production, called lulls (Armstrong, 1988; Ducea et al., 2015a; Kirsch et al., 2016; Paterson and Ducea,

2015). The pattern or pace of this episodic behavior is called an “arc tempo” and occurs at spatial and temporal scales ranging from individual volcanic buildups to the assembly and dispersal of supercontinents (Cao et al., 2017; de Silva et al., 2015; Ducea et al., 2015a; Paterson and Ducea, 2015). In this contribution, we focus on magmatic flare ups that occur at intervals of a few 10s of millions of years to several 10s of millions of years (Ducea et al., 2015a; Kirsch et al., 2016; Paterson and Ducea, 2015) and affect large segments of continental arc

\* Corresponding author.

E-mail address: [jay.chapman@uwyo.edu](mailto:jay.chapman@uwyo.edu) (J.B. Chapman).

<https://doi.org/10.1016/j.lithos.2021.106307>

Received 1 March 2021; Received in revised form 16 June 2021; Accepted 16 June 2021

Available online 19 June 2021

0024-4937/© 2021 Elsevier B.V. All rights reserved.

systems, up to 1000s of km along strike. What causes flare ups and episodic behavior in subduction systems is among the most fundamental, outstanding questions in the Earth Sciences (Huntington et al., 2018; Yoder et al., 2020). Understanding the origin of flare ups is consequential for many reasons, including evaluating the causes of long-term climate change (e.g., Cao et al., 2017; Lee and Lackey, 2015; McKenzie et al., 2016; Ratschbacher et al., 2019), explaining the distribution of natural resources (e.g., Sillitoe, 2018; Yang and Santosh, 2015), and deciphering the geodynamics of convergent margins (e.g., DeCelles et al., 2009).

Mesozoic and younger examples of continental arc systems that exhibit episodic magmatic behavior include the Coast Mountains batholith (e.g., (Gehrels et al., 2009); Beranek et al., 2017; Cecil et al., 2018), North Cascades arc (e.g., Shea et al., 2018), Sierra Nevada batholith (e.g., Attia et al., 2020; Ducea, 2001), Peninsular Ranges batholith (e.g., Jiang and Lee, 2017; Kistler et al., 2003, 2014), Trans-Mexican belt (e.g., Cavazos-Tovar et al., 2020; Ferrari et al., 2002), Panama-Colombian arc (e.g., Cardona et al., 2018; Rodríguez et al., 2018), Ecuadorian arc (e.g., Schütte et al., 2010), Peruvian Coastal batholith (e.g., Martínez-Ardila et al., 2019a), central Andean arc (e.g., DeCelles et al., 2009, 2015), Chilean Coastal batholith (e.g., Martínez-Ardila et al., 2019a), North Patagonia batholith (e.g., Gianni et al., 2018), Antarctic Peninsula to Marie Byrd Land (e.g., Riley et al., 2018), Median batholith in New Zealand (e.g., Schwartz et al., in press), Sumatran arc (e.g., Zhang et al., 2019a, 2019b), Wuntho-Popa arc in Myanmar (e.g., Licht et al., 2020); Gangdese batholith (e.g., Ji et al., 2009; Kapp and DeCelles, 2019), South Pamir batholith (e.g., Chapman et al., 2018); Urumieh–Dokhtar belt in Iran (e.g., Chaharlang et al., 2020; Sepidbar et al., 2018), Anatolian volcanic province (e.g., Schleiffarth et al., 2018), South China continental arc (e.g., Li et al., 2012), Korean Peninsula (e.g., Cheong and Jo, 2020), and Kamchatka arc (e.g., Akinin et al., 2020). Many Paleozoic (e.g., Famatinian arc, Argentina; Otamendi et al., 2012; the Anti-Atlas; Triantafyllou et al., 2020) to Late Proterozoic (e.g., Cadomian arc, Iran, Moghadam et al., 2017; West Gondwana, Ganade et al., 2014, 2021) examples also exist. These examples are chiefly associated with strongly convergent or advancing Cordilleran orogenic systems, which distinguishes them from retreating or extensional subduction zones that are characterized by long-term slab rollback, upper plate extension, and the formation of new oceanic crust (e.g., Tasmanides; Cawood et al., 2009; Kemp et al., 2009). Often referred to as “accretionary orogens” (Glen, 2013; Rosenbaum, 2018), these systems exhibit increased magmatic activity during periods of slab rollback and extension, but “flare up” terminology is generally not used when describing them (Collins, 2002; Collins and Richards, 2008).

The term “flare up” is commonly used to describe two different magmatic processes in strongly convergent Cordilleran orogens that both operate on similar time scales, a few millions of years to several tens of millions of years, leading to confusion. The original usage of “flare up” describes the eruption of large volumes of silicic ignimbrites in orogenic interiors, far inland from the plate margin (Lipman et al., 1971; Noble, 1972). In this scenario, the distinction between arc and back arc is lost and magmatic activity occurs across a very broad area, up to several hundred km inland from the trench (Best et al., 2016). These flare ups are often associated with continental plateau formation, slab roll-back, delamination, and/or extension (Best et al., 2009; Farmer et al., 2008; Ferrari et al., 2002). The Neogene ignimbrite flare up in the Altiplano-Puna orogenic plateau (e.g., de Silva and Kay, 2018) and the mid-Cenozoic ignimbrite flare up in North America (e.g., Best et al., 2016) are well-known examples. The second type of flare up, and the focus of the present review, occurs in the primary or frontal arc of Cordilleran orogens and is thought to lead to the development of large coastal batholiths and mafic-to-ultramafic residual assemblages (e.g., Ducea, 2001). The term “high-flux episode” or “high-flux event” is sometimes used to help distinguish arc flare ups from ignimbrite-type flare ups (DeCelles et al., 2009), but the terms all continue to be used interchangeably throughout the literature. Despite the geodynamic

differences between the two types of flare ups, there may be petrogenetic similarities, which are discussed in Section 8.

Episodic patterns of magmatic activity have long been recognized in Cordilleran orogenic systems (e.g., Armstrong, 1988; Coira et al., 1982), but there was a resurgence of interest in continental arc tempos when flare ups were observed to coincide with a shift to more evolved radiogenic isotopic compositions, which was hypothesized to have been caused by underthrusting of melt-fertile continental lithosphere into the arc source region (Ducea, 2001; Ducea and Barton, 2007; Haschke et al., 2002a, 2002b). This hypothesis was subsequently developed into a conceptual model, called the “Cordilleran cycle,” that links arc flare ups with a series of upper plate processes in Cordilleran orogens, including contractional to extensional deformation of orogenic interiors, propagation of the retroarc thrust belt, foreland basin development, arc root delamination, crustal thickening, surface uplift, forearc subsidence, and accretionary wedge exhumation (DeCelles et al., 2009, 2015; DeCelles and Graham, 2015; Ducea et al., 2015a). This model, and its emphasis on the feedbacks between magmatism, tectonics, and lithospheric evolution, is highly influential in the tectonics community, but has been challenged by a number of recent studies that present new or evolving views on the causes and nature of arc flare ups and magmatic lulls (Cope, 2017; Decker et al., 2017; Ducea et al., 2017; Cecil et al., 2019; Chapman and Ducea, 2019; Martínez-Ardila et al., 2019a; Attia et al., 2020; Klein et al., 2021; Yang et al., 2020; Schwartz et al., in press).

Besides the Cordilleran cycle model, few studies have presented physical processes or mechanisms that can explain what causes episodic behavior across multiple arc systems. A commonly cited alternative is that semi-episodic changes in plate convergence rates may cause flare ups and magmatic lulls (Hughes and Mahood, 2008; Zellmer, 2008), although where available, data do not support this hypothesis (e.g., Cecil et al., 2018; DeCelles et al., 2009; Ducea, 2001; Kirsch et al., 2016; Zhang et al., 2019a, 2019b). Other alternatives include underplating related to subduction erosion (e.g., Chapman et al., 2013, 2014; Kay et al., 2005), arc migration (Chapman and Ducea, 2019), and punctuated melt extraction from the lower crust (Ducea et al., 2020b). Many additional factors affect magma production rates in subduction systems, including volatile release from the slab, mantle convection rates, and the height of the mantle wedge above the slab (e.g., Plank and Langmuir, 1988; Turner and Langmuir, 2015). These factors have been listed as possibilities to explain flare ups and lulls (e.g., Chapman and Ducea, 2019; Martínez-Ardila et al., 2019a), but they have not been rigorously evaluated as a driver of arc tempos.

All magmatic flare ups are unique on some level and there are numerous processes that have been proposed to explain individual arc flare ups. We focus on commonalities between arc systems and the mechanisms that can explain flare ups in multiple continental arcs. Perhaps all flare ups are singular, “one-off,” events in Earth history, but temporal patterns and shared characteristics suggest that many flare ups could have a common cause. In the first part of this review, we examine convergent continental arcs globally to evaluate what that common cause may be. In the second part of this review, we investigate the role of arc migration in modulating magma production rates. Flare ups may also occur in stationary, non-migrating, continental arcs (e.g., Jurassic Sierra Nevada arc; Chen and Moore, 1982; Cecil et al., 2012), in which case additional processes may be needed, which are not explored here. The paper concludes with the presentation of a conceptual model that explores how flare ups and magmatic lulls could be related to arc migration and discusses how this concept can be integrated into existing geodynamic models.

## 2. Definitions and characteristics of flare ups

There is no universally agreed-upon definition or threshold for a magmatic event to be called a “flare up,” in large part because episodic magmatic activity in continental arcs occurs at a wide range of spatial and temporal scales (de Silva et al., 2015) and is never steady-state. In

this review, we focus on flare ups that are approximately synchronous for 100 s to 1000s of km along strike in continental arc systems (e.g., Cretaceous flare up in the Peninsular Ranges batholith; Kistler et al., 2014). Detailed studies of smaller arc segments reveal greater variation in periods of increased magmatic activity that may be unique to that segment or be temporally offset from neighboring segments (e.g., Coast Mountains batholith; Cecil et al., 2018). This suggests that flare ups are rarely ever truly synchronous over long distances and helps to explain, in part, the difficulty in comparing the duration of flare ups from one arc system to the next, or from one study to another. This also suggests that reported flare up duration should scale with the length of the arc

segment considered. For example, Zhang et al. (2019a, 2019b) estimated the Paleogene flare up event for the entire Neo-Tethyan margin (ca. 6000 km) to have lasted ~25 Myr, whereas the same flare up event in Sumatra (ca. 500 km arc length) lasted ~5 Myr. On average, studies of continental arc systems that have produced flare up events report flare up durations from 10 to 25 Myr (see Fig. 1 for a compilation). Detailed geochronological studies (e.g., zircon U—Pb CA-TIMS) of flare ups in arc segments suggest that the bulk of flare up magmatism is emplaced within even shorter time scales (< 5 Myr) (e.g., Median batholith, Schwartz et al., 2017; Famatinian arc, Ducea et al., 2017). However, the methods employed to define flare up duration varies from study to study

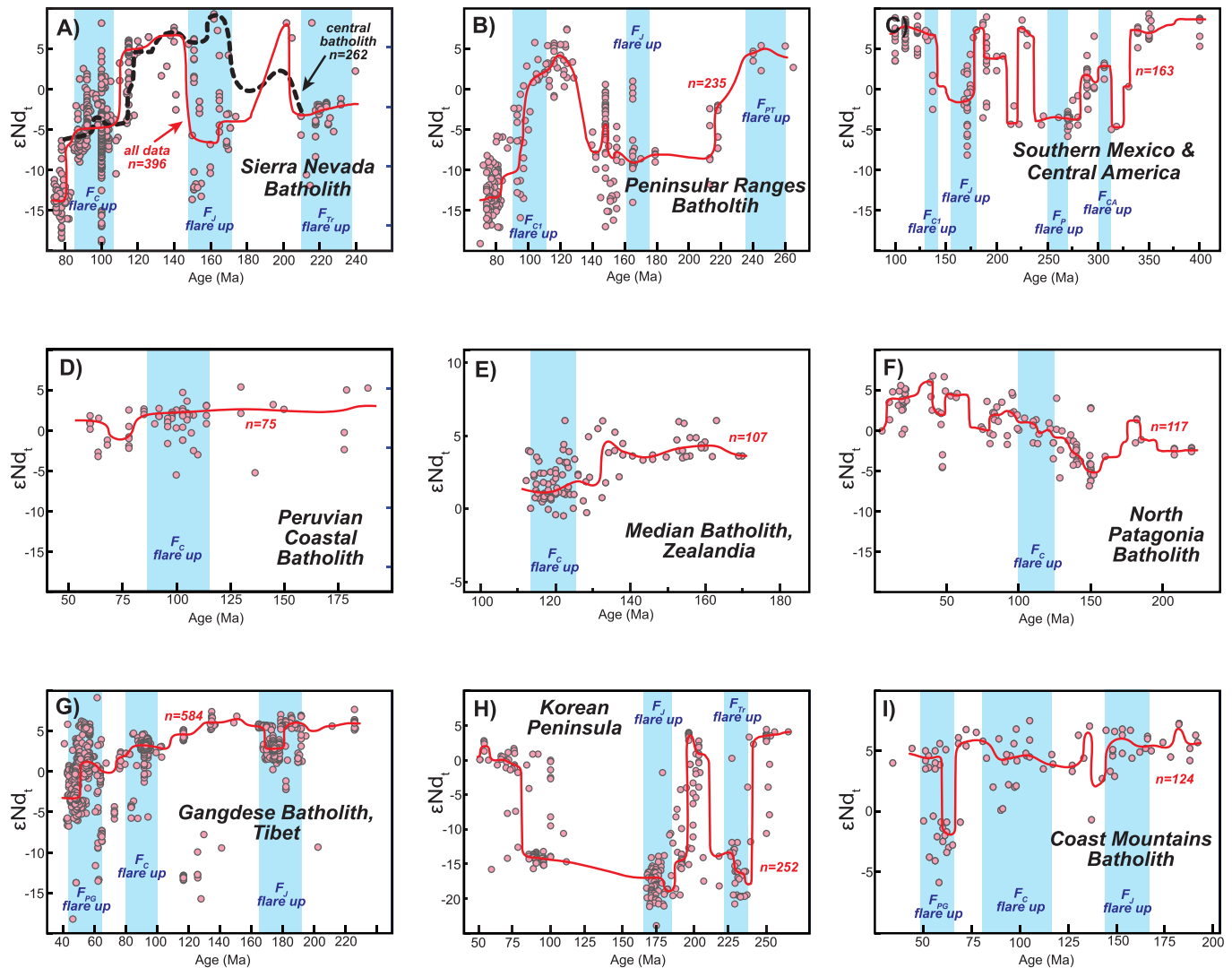


**Fig. 1.** Age-corrected, initial radiogenic isotopic compositions for igneous rocks in continental arc segments (pink circles). Red lines are running medians of bivariate kernel density estimates (Sundell et al., 2019). A) Data from the entire Sierra Nevada batholith (pink circles and solid line; Kirsch et al., 2016) compared to the central Sierra Nevada batholith (37.5–38.13°N latitude, dashed line), compiled by Ardill et al. (2018).  $F_C$ ,  $F_J$ , and  $F_{TR}$  (vertical blue-colored bands) refer to the Cretaceous, Jurassic, and Triassic flare ups, respectively and are based on flare up intervals identified in Kirsch et al. (2016). B) Data from the Peninsular Ranges batholith and northwestern Mexico plotted with the mid-Cretaceous ( $F_{C1}$ ), Jurassic ( $F_J$ ), and the Permian-Triassic ( $F_{PT}$ ) flare ups. Modified from Kirsch et al. (2016). C) Data from southern Mexico and northern Central America plotted with the Early Cretaceous ( $F_{C1}$ ), Jurassic ( $F_J$ ), Permian ( $F_P$ ), and Carboniferous ( $F_{CA}$ ) flare ups. Modified from Kirsch et al. (2016). D) Data from the Peruvian Coastal batholith showing the Cretaceous flare up ( $F_C$ ), modified from Martinez-Ardila et al. (2019a) and references therein. E) Whole rock  $\epsilon Nd(t)$  data and average sample zircon Hf isotope data, converted to  $\epsilon Nd(t)$  using the terrestrial array of Vervoort et al. (1999), for the Median batholith. Data compilation and timing of the Cretaceous flare up ( $F_C$ ), is from Milan et al. (2017), Schwartz et al. (in press), and references therein. F) Data from the North Patagonia batholith showing the Cretaceous flare up ( $F_C$ ), compiled from Echaurren et al. (2019) and references therein. G) Data from the central Gangdese batholith plotted with the Paleogene ( $F_{PG}$ ), Cretaceous ( $F_C$ ), and Jurassic ( $F_J$ ) flare ups, compiled from Chapman and Kapp (2017). H) Data from the Korean Peninsula plotted with the Jurassic ( $F_J$ ) and Triassic ( $F_{TR}$ ) flare ups, compiled from Kim et al., 2016, 2020, Cheong and Jo (2020), and references therein. I) Data from the central and southern Coast Mountains batholith (Ducea and Barton, 2007; Girardi et al., 2012) and references therein. Data includes average sample zircon Hf isotope values from Cecil et al. (2011) converted to  $\epsilon Nd(t)$  using the terrestrial array of Vervoort et al. (1999). The Paleogene ( $F_{PG}$ ), Cretaceous ( $F_C$ ), and Jurassic ( $F_J$ ) flare ups are adopted from Cecil et al. (2018) for the southern and central segments of the batholith.

and there is no standardized method for constraining how long flare ups last. Most of the studies examined as part of this review report flare up duration based on a range of ages in which the majority of age data are located (e.g., using histograms or density functions). Mathematically, this is roughly equivalent to reporting standard deviation from normally distributed age populations, which does not include age distribution “tails” within the reported flare up duration. In addition, the method used to define the “majority” of age data (e.g.,  $1\sigma$  or  $2\sigma$ ) is rarely reported. Similar to flare ups, the durations of magmatic lulls are ill-defined, and have been reported to last anywhere from 5 to 70 Myr in arc systems that experienced multiple flare ups (Fig. 1). Future research into the duration of flare ups and lulls, scaled with the length of arc segments, will be a fruitful avenue of inquiry.

Continental arcs that have experienced multiple flare ups generally exhibit episodic behavior at intervals of 25–80 Myr (Fig. 1), which is a slightly larger range than reported in previous compilations (30–70 Myr, DeCelles et al., 2009; Paterson and Ducea, 2015). Unlike flare up duration, the interval between flare ups is more easily defined using peak positions in age populations. Some previous studies have suggested that repeated flare ups may be truly periodic, occurring at regular intervals of time, which has also been called cyclical magmatism (DeCelles et al., 2009). However, more recent studies have shown that repeated flare up events are rarely, if ever, periodic, and are more accurately described as episodic, reoccurring at irregular intervals of time (Paterson and Ducea, 2015; Kirsch et al., 2016; this study). The term “cyclical” to describe repeated flare ups is problematic because it implies periodicity and the term is now widely used to describe a chain of events or processes that may lead to an arc flare up (e.g., the Cordilleran cycle, Andean cycle, Wilson cycle), but which do not necessarily produce periodic arc behavior. Thus, we reserve the term cyclical to describe tectonic or geodynamic models that incorporate a repeating series of linked processes and use the term episodic to describe arc tempos in general.

Continental arc flare ups are generally defined using either age data alone or magmatic addition rates. In this study, we employ magmatic addition rates to compare flare ups and exclusively report “bedrock” igneous rock ages (i.e., not detrital geochronological data). The term magmatic addition rate has been defined in various ways in the past (see review in Paterson and Ducea, 2015), but is used here as an all-inclusive term for any calculation that combines volumetric and age data. There are four main types of magmatic addition rates in common usage (Table 1). The first is an areal addition rate, which has the units  $\text{km}^2 \text{Myr}^{-1}$  and is calculated using the areal (map-view) extents of arc rocks. Cecil et al. (2018) provide a comprehensive description on the methodology for this method. The second type is a volume addition rate that has units of  $\text{km}^3 \text{Myr}^{-1}$  and is calculated using both areal and depth extents (or estimates) of arc rocks. Constraints on depth extents can be estimated from tilted arc crustal sections, geophysical data, or other independent datasets (e.g., Crisp, 1984). The third and fourth types of magmatic addition rates normalize volume addition rates using arc length (parallel to trench) alone or using both arc length and arc width (perpendicular to trench). Volume addition rates normalized by arc length have the units  $\text{km}^3 \text{km}^{-1} \text{Myr}^{-1}$ , are the most widely reported type of magmatic addition rate (Reymer and Schubert, 1984; Gehrels et al., 2009; Jicha and Jagoutz, 2015; Paterson and Ducea, 2015; de Silva and Kay, 2018), and is used throughout this paper. Rates reported in previous publications with different units are converted for comparison purposes. The units  $\text{km}^3 \text{km}^{-1} \text{Myr}^{-1}$  are sometimes referred to as an Armstrong unit (AU), and for arc crust production,  $1 \text{ AU} = 30 \text{ km}^3 \text{km}^{-1} \text{Myr}^{-1}$  (DeCelles et al., 2009). Ratschbacher et al. (2019) recognized that arc width is not constant throughout the life of an arc system (e.g., Cao et al., 2017) and normalized volume addition rates by arc length and arc width, with the units  $\text{km}^3 \text{km}^{-2} \text{Myr}^{-1}$ . Arc width varies from arc to arc and throughout time, but the global average is ca. 100 km (de Bremond d’Ars et al., 1995).

Regardless of the type of magmatic addition rate employed, the most robust estimates consider the effects of erosion and deformation –

**Table 1**  
Definitions of key terms and rates.

Magmatic Addition Rates			
Name	Units	Notes	Key References
Areal addition rate	$\text{km}^2 \text{Myr}^{-1}$	Calculated from areal extents, “map-view,” only	Ducea, 2001; Cecil et al., 2018
Volume addition rate	$\text{km}^3 \text{Myr}^{-1}$	Calculated from areal extents and depth estimates	Gehrels et al., 2009
Volume addition rate per arc length (“Armstrong Unit”)	$\text{km}^3 \text{km}^{-1} \text{Myr}^{-1}$	Volume addition rate normalized by arc length	DeCelles et al., 2009; Jicha and Jagoutz, 2015; Paterson and Ducea, 2015; de Silva and Kay, 2018
Volume addition rate per area	$\text{km}^3 \text{km}^{-2} \text{Myr}^{-1}$	Volume addition rate normalized by arc length and arc width	Ratschbacher et al., 2019
Other Rates			
Name	Description		
Arc crust production rate	Magmatic addition rate used to describe long-term production of arc rocks that includes mantle-derived rocks as well as incorporation of pre-existing crustal rocks.		
Continental crust formation rate	Rate used to describe the long-term creation of new continental crust. Only includes mantle-derived rocks. Similar to arc crust production rate if effects of crustal assimilation/contamination are removed.		
Mantle-derived melt production rate	Volume addition rate used to describe mantle-derived melts. Includes rocks that are returned to the mantle (e.g., arc root foundering) and do not contribute to the long-term arc crust or continental crust record.		

resulting in changes in arc dimensions, magmatic activity from the forearc to the backarc, and contributions from both volcanic and intrusive magmatism (e.g., Jicha and Jagoutz, 2015; Ratschbacher et al., 2019). For continental arc flare ups, magmatic addition rates are most commonly used to describe all igneous arc rocks, regardless of whether the rocks were produced from the mantle or reworking of pre-existing crust (e.g., Paterson and Ducea, 2015). We refer to this usage as arc crust production rate (see Section 6 and Table 1). Arc crust production is different from continental crust formation (e.g., Jagoutz and Kelemen, 2015), which only considers mantle-derived additions to the crust. The fraction of arc crust produced by the mantle has been called a mantle-derived magmatic addition rate (e.g., Ratschbacher et al., 2019). We introduce a new term, mantle-derived melt production rate (see Section 7), to describe the amount of melt produced in the mantle wedge, inclusive of the asthenospheric and lithospheric mantle. This term is different from mantle-derived magmatic addition rate because it includes all melt/magma generation, not just the fraction of that melt/magma that becomes a “permanent” part of the continental crust. The most significant difference between the two terms is the inclusion of arc rocks that are recycled back into the mantle, chiefly by delamination of arc roots, in mantle-derived melt production rates. This value (mantle-derived melt production rate) was called magmatic addition/production for intraoceanic island arc systems by Jicha and Jagoutz (2015), but we avoid that term to prevent confusion with other magmatic addition rate terminology.

### 3. Radiogenic isotopes and the role of the mantle

Changes in the radiogenic isotopic composition of magmatism during arc flare ups have been one of the most closely examined aspects of the Cordilleran cycle model. A key tenet of the model is that continental arc magmatism shifts to more evolved isotopic compositions (e.g., more negative  $\epsilon\text{Nd}$  and  $\epsilon\text{Hf}$ , more positive  $^{87}\text{Sr}/^{86}\text{Sr}$ ) during flare ups, which is

attributed to retroarc underthrusting and introduction of isotopically evolved, melt-fertile continental crust or lithosphere into the arc source region (DeCelles et al., 2009, 2015; DeCelles and Graham, 2015; DePaolo et al., 2019; Ducea, 2001; Ducea and Barton, 2007). Arcs constructed on juvenile lithosphere, like young accreted terranes (e.g., Coast Mountains batholith; Wetmore and Ducea, 2011; Girardi et al., 2012; Cecil et al., 2019), are not expected to exhibit the same isotopic shift.

As more isotopic and geochronologic data becomes available, it is apparent that there is great variability in the temporal radiogenic isotopic patterns associated with flare ups. While some studies suggest that flare ups coincide with shifts to more evolved isotope ratios (e.g., Cretaceous Sierra Nevada batholith, Cretaceous Peninsular Ranges batholith, Cretaceous Median batholith, Jurassic and Triassic arcs in the Korean Peninsula, Eocene Gangdese batholith, Paleogene Coast Mountains batholith) (Fig. 1), other flare ups occur with little to no change in isotopic composition (e.g., Cretaceous and Jurassic Coast Mountains batholith, Cretaceous Peruvian Coastal batholith, Cretaceous North Patagonia batholith; Jurassic Peninsular Ranges batholith) (Fig. 1). Some temporal isotopic shifts are observable throughout the entire arc, while others may only affect certain arc segments (e.g., Jurassic flare up in the Sierra Nevada batholith; Cecil et al., 2012; Ardill et al., 2018; Fig. 1A). Flare ups are often associated with an increase in the range of measured isotope ratios, but the average isotopic composition may not significantly change, indicating that there may be isotopic excursions toward both more evolved and more juvenile values during a flare up (e.g., Fig. 1A). These data suggest that melting of ancient, highly evolved crustal material may not be required to produce a flare up.

Even if melt-fertile crustal material was necessary to produce a flare up, it is uncertain if that material can be introduced into the melt source region rapidly enough. Yang et al. (2020) modeled lower crustal melting at a constant rate of retroarc underthrusting and concluded that not enough magma is produced to explain the high rates of magma addition observed during flare ups in Cordilleran orogenic systems analogous to the Cretaceous Sierra Nevada arc and Sevier retroarc thrust belt. Besides retroarc underthrusting (e.g., DeCelles et al., 2009), sediment subduction/accretion has been proposed as a mechanism to deliver crustal material into an arc system and produce a flare up and isotopic shift (Chapman et al., 2013; Ducea and Chapman, 2018; Kay et al., 2005; Straub et al., 2020). Sediment subduction can introduce large volumes of crustal material into the subarc mantle at comparatively rapid rates (Clift and Vannucchi, 2004). One issue with this hypothesis is that trench and forearc sediments may be too juvenile to explain the shift to more evolved isotopic compositions (Chapman et al., 2017; Ducea et al., 2015b). For example, an isotopically evolved component  $< -10 \text{ } \epsilon\text{Nd}_{(t)}$  in the source region is required to explain the composition of the Cretaceous Sierra Nevada batholith (Ducea, 2001; Ducea and Saleeby, 1998), but trench, accretionary complex, and forearc rocks are predominantly  $\geq 0 \text{ } \epsilon\text{Nd}_{(t)}$  (King et al., 2006; Linn et al., 1992; Nelson, 1995). Nevertheless, sediment subduction remains an underexplored possibility to explain many arc flare ups. Another possibility is that downward flow within the arc could introduce isotopically evolved crustal rocks into the source region (Cao et al., 2016; Paterson and Farris, 2008). Studies of inherited volcanic zircon in deeply emplaced ( $\sim 5 \text{ kbar}$ ) intrusive rocks in the Sierra Nevada suggest that downward flow may be relative rapid, on the order of 1 Myr (Saleeby, 1990), although the volume of magma generated by this process remains to be rigorously evaluated.

Several recent isotopic studies have documented continental arc flare ups (e.g., Sierra Nevada batholith, Andean coastal batholiths, Gangdese batholith, North China arc, Median batholith, Famatinian arc) that do not require extraordinary assimilation of continental crust or sediments and are instead, chiefly derived from the mantle (Zhu et al., 2009; Cope, 2017; Decker et al., 2017; Ducea et al., 2017; Cecil et al., 2019; Martinez-Ardila et al., 2019a; Alasino et al., 2020; Attia et al., 2020; Dafov et al., 2020; Klein et al., 2021; Schwartz et al., in press).

These findings are largely based on assimilation and crystallization models that require an isotopically juvenile component to explain the range of isotopic compositions produced during a flare up and geochemical data that suggests the juvenile component is the mantle (e.g., Martinez-Ardila et al., 2019a). The juvenile component in the source could be the depleted mantle (i.e., asthenospheric mantle wedge; Schwartz et al., 2017; Martinez-Ardila et al., 2019a; Attia et al., 2020) or the mantle lithosphere (Chapman et al., 2017; Chapman and Ducea, 2019). We propose that the mantle lithosphere is an important source of mantle-derived melts during flare ups.

Even the least differentiated (e.g., high Mg #, low  $\text{SiO}_2$ ) continental arc rocks produced during flare ups do not exhibit depleted mantle isotopic compositions (e.g.,  $\epsilon\text{Hf}_{(0)} = +15$ ,  $\epsilon\text{Nd}_{(0)} = +10$ ,  $^{87}\text{Sr}/^{86}\text{Sr}_{(0)} = 0.703$ ; where the subscript  $(0)$  indicates present-day values) in arcs where the upper plate is continental and relatively old, which has been interpreted to reflect a lithospheric mantle source for flare up magmas (Chapman et al., 2017). For example,  $^{87}\text{Sr}/^{86}\text{Sr}_{(0)}$  ratios of Jurassic to Paleogene age intrusive rocks from the Coast Mountains batholith are higher (more evolved) than depleted mantle values, show no correlation with  $\text{SiO}_2$ , and do not significantly change with increasing depth in the arc (Girardi et al., 2012; Ducea, unpublished data) (Fig. 2). Tilted crustal sections in the Famatinian arc, Salinian arc, and southern Sierra Nevada batholith also expose deep arcs rocks and the most primitive rocks, mafic cumulates and gabbro, are 5–20  $\epsilon\text{Nd}$  or  $\epsilon\text{Hf}$  units more evolved than depleted mantle values (Pickett and Saleeby, 1994; Kidder et al., 2003; Otamendi et al., 2012; 2017; Chapman et al., 2014; Alasino et al., 2016, 2020; Ducea et al., 2017; Klein et al., 2021; Klein and Jagoutz, 2021). Likewise, garnet pyroxenite xenoliths interpreted as residual assemblages, “arclogites,” from the Sierra Nevada have relatively evolved ( $\epsilon\text{Nd}_{(t)} < 0$ ) compositions (Ducea and Saleeby, 1998; Ducea, 2002; Ducea et al., 2020a). These observations support a mantle lithosphere source for several Cordilleran arc magmas, which can subsequently assimilate pre-existing crust. Many generalized models for arc magmatism focus exclusively on the role of the asthenospheric mantle wedge (e.g., Grove et al., 2012), but the isotopic data are most consistent with a primary origin for continental arc magmas in the lithospheric mantle during flare ups (Fig. 3). Importantly, the roots of four main arcs, where mafic rocks with low  $\text{SiO}_2$  and high MgO are available (Sierra Nevada, Salinia, Famatinia, and Coast Mountains) all show similar radiogenic isotopic compositions from gabbros to granites, from the deepest exposed to the shallowest levels of the crust, which suggests that the mantle source region for these rocks is not chiefly depleted asthenospheric mantle. This is a major problem for models that envision melting

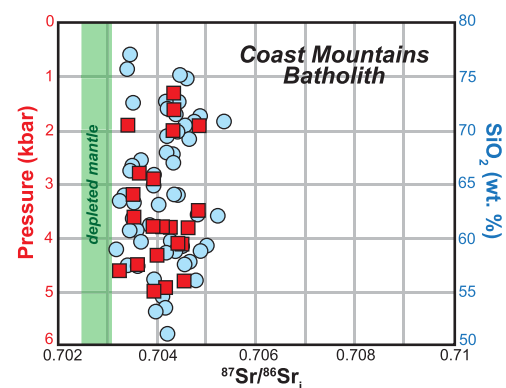
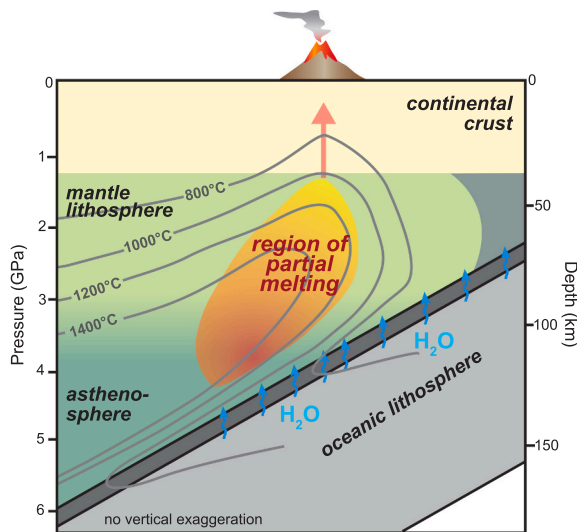


Fig. 2. Initial (age-corrected), whole rock  $^{87}\text{Sr}/^{86}\text{Sr}$  isotope ratios from the Coast Mountains batholith are relatively constant with pressure/depth (red squares) and show no correlation with  $\text{SiO}_2$  (blue circles). This suggests that the isotopic values were acquired from the source region, which is interpreted to be the mantle lithosphere because  $^{87}\text{Sr}/^{86}\text{Sr}$  values are higher than the depleted mantle. Data is from Girardi et al. (2012) and includes Jurassic to Paleogene intrusive arc rocks.



**Fig. 3.** A schematic cross-section of a subduction zone showing how the mantle lithosphere may be incorporated into the mantle wedge and contribute melt to the arc system. Isotherms and the region of dehydration are adopted from Schmidt and Poli (1998). Many schematic cross-sections for mantle melting (e.g., Grove et al., 2012; their Fig. 6a) do not distinguish between lithospheric and asthenospheric mantle. The lithosphere-asthenosphere boundary is blurred because it is, in-part, thermally controlled (e.g., Niu, 2021).

in the asthenospheric mantle wedge is the primary driver of mantle-derived magmatism in arc systems (Davies and Stevenson, 1992; Katz et al., 2003; Grove et al., 2012).

Chapman et al. (2017) proposed that the shift to more evolved radiogenic isotopes that is commonly associated with flare ups is related to landward arc migration (see Section 10 below) and a change from asthenospheric mantle sources near the trench to more lithospheric mantle sources away from the trench (landward). The complementary trend – more juvenile magmas produced during trenchward migration is also observed in arcs (e.g., mid-Cretaceous Kohistan arc; Bouilhol et al., 2011), but not discussed here. The more evolved isotopic values located farther from the trench reflect more ancient lithospheric provinces, including older mantle lithosphere. Recent studies from the Median batholith, Sierra Nevada batholith, and Coast Mountains batholith have tested this idea (Attia et al., 2020; Cecil et al., 2019; Decker et al., 2017; Schwartz et al., in press). These batholiths exhibit shifts to more evolved radiogenic isotope ratios during a flare up, concurrent with landward arc migration (Ducea, 2001; DeCelles et al., 2009; Gehrels et al., 2009; Girardi et al., 2012; Milan et al., 2017). However, when magmatism is examined from a more narrowly defined geographic region within the arc, isotopic ratios remain unchanged or even become slightly more juvenile during flare ups (Attia et al., 2020; Cecil et al., 2019; Schwartz et al., in press), inconsistent with the batholith-wide trends. For example, apart from a few clusters of analyses, igneous rocks from the Ritter Range pendant in the Sierra Nevada batholith have a narrow range of isotopic compositions (0 to +5 zircon  $\epsilon\text{Hf}_{(t)}$ ) throughout the Mesozoic with slightly more juvenile isotopic compositions toward the present (Attia et al., 2020) (Fig. 4). This is in contrast to data compiled from the entire batholith, which reveal larger isotopic shifts (+5 to –10  $\epsilon\text{Nd}_{(t)}$ ) between flare ups and lulls (Ducea, 2001; Ducea and Barton, 2007; Kirsch et al., 2016) (Fig. 4). One possibility is that the larger data compilations are averaging batholith-wide variations and the comparisons to geographically focused regions are not appropriate. Another possibility is that this discrepancy between geographically focused studies and batholith-wide studies indicates that shifts to more evolved isotopic compositions observed during flare ups are a function of the position of the arc axis relative to the upper mantle and deep lithospheric architecture at that position, rather than changes in the magma

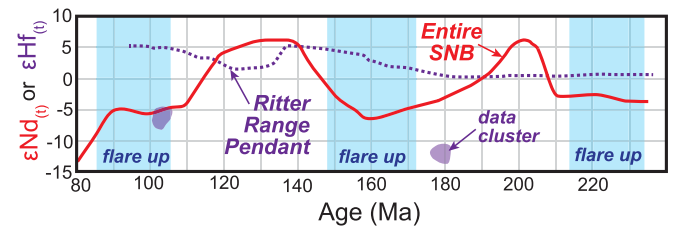


**Fig. 4.** A comparison of temporal isotopic trends in zircon  $\epsilon\text{Hf}_{(t)}$  data (dashed purple line, based on 31 rock samples, 654 individual zircon analyses) from the Ritter Range pendant in the Sierra Nevada batholith (SNB) with whole rock  $\epsilon\text{Nd}_{(t)}$  data (red solid line, based on 392 rock samples) from the entire Sierra Nevada batholith. Data from Kirsch et al. (2016) and Attia et al. (2020).

source region (e.g., Kistler, 1990). The model of Chapman et al. (2017) predicts that when magmatism is only considered from a single position in the arc/batholith, the isotopic composition of magmatism will not significantly change through time. This model is supported by studies of crustal sections through arcs, which show limited isotopic variation from the arc root (arclogites) to the upper crust (Ducea, 2002; Girardi et al., 2012; Otamendi et al., 2012; 2017; Klein et al., 2021). Additional support for the role of arc migration in producing temporal isotopic trends comes from detailed studies that show the shift to more evolved radiogenic isotopic compositions can begin 10s of Myr before a flare up starts (e.g., Korean Peninsula, Cheong and Jo, 2020) (Fig. 5).

#### 4. Oxygen isotopes and crustal contributions

Radiogenic isotopes can help distinguish between asthenospheric mantle and lithospheric mantle sources, but stable oxygen isotopes are better suited to identifying crustal and mantle contributions to arc magmatism (Taylor Jr., 1978). Partial melting of the mantle produces mafic melts with  $\delta^{18}\text{O}$  values of 5–6‰, which remain near constant during crystal fractionation (Bucholz et al., 2017; Eiler, 2001). Zircon that crystallized in equilibrium with a mantle melt has similar  $\delta^{18}\text{O}$  values, 5–6‰, and quartz that crystallized after some amount of fractionation has slightly elevated values of 6–7‰ (Valley, 2003), due to isotope fractionation. There does not appear to be a systematic change (i.e., common to multiple arc systems) in  $\delta^{18}\text{O}$  during flare up events, however, more detailed studies comparing trends in bulk rock, zircon, quartz, and other minerals are needed. For example, the Peninsular Ranges batholith exhibits a shift toward higher bulk rock  $\delta^{18}\text{O}$  during

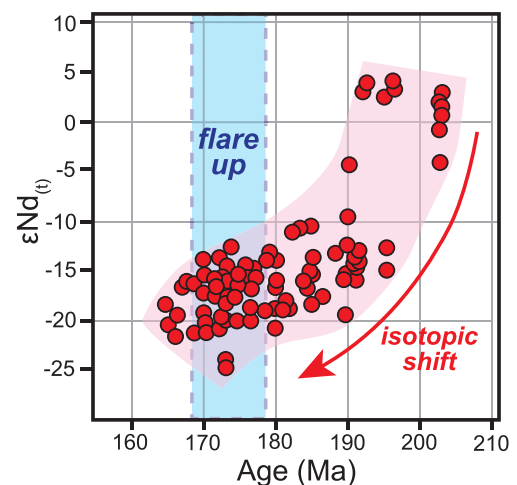


**Fig. 5.** The shift toward more evolved radiogenic isotopic values in Jurassic arc rocks on the Korean Peninsula started 20–30 Myr before the magmatic flare up at ca. 175 Ma. The isotopic shift is concurrent with landward arc migration (Fig. 10D). Data from Cheong and Jo (2020).

the Late Cretaceous flare up (Kistler et al., 2014; Silver and Chappell, 1988), the Sierra Nevada batholith exhibits a shift toward lower bulk rock and zircon  $\delta^{18}\text{O}$  during the Late Cretaceous flare up (Lackey et al., 2008), and the Coast Mountains batholith does not exhibit any clear temporal shift in quartz  $\delta^{18}\text{O}$  during the Late Cretaceous to Paleogene flare up (Wetmore and Ducea, 2011) (Fig. 6A–C). Many continental arcs, including the Median batholith, Peninsular Ranges batholith, and Sierra Nevada batholith, also exhibit pronounced across-arc spatial trends in  $\delta^{18}\text{O}$ , which have been interpreted to reflect lithospheric provinces and basement terranes at the largest spatial scales (Kistler et al., 2014; Lackey et al., 2008; Schwartz et al., in press). This suggests that the temporal  $\delta^{18}\text{O}$  trends in these arcs are at least partially controlled by arc migration across lithospheric boundaries.

In detail, however, the temporal record of  $\delta^{18}\text{O}$  in these arcs reflect a variety of processes and diverse petrogenetic mechanisms. For instance, the shift toward higher zircon  $\delta^{18}\text{O}$  in the Median batholith (Fig. 6D) has been interpreted to reflect landward arc migration from hydrothermally altered accreted terrane basement to peri-cratonic Gondwanan lithosphere (Schwartz et al., in press). Superimposed on that trend is a pulse of sediment subduction and melting during the mid-Cretaceous flare up that further increased zircon  $\delta^{18}\text{O}$  (Decker et al., 2017; Schwartz et al., in press). In addition to basement composition, the landward decrease in the spatial  $\delta^{18}\text{O}$  trend from the Sierra Nevada batholith was interpreted by Lackey et al. (2008) to be caused by increased melting of lithospheric mantle, coincident with the Late Cretaceous flare up. In some cases, it is difficult to determine whether temporal  $\delta^{18}\text{O}$  shifts have any relationship to flare ups at all. The Late Paleozoic to Early Mesozoic Chilean Coastal and Frontal batholiths display a long-term (> 100 Myr) temporal trend toward lower  $\delta^{18}\text{O}$  that encompasses multiple flare up events (del Rey et al., 2016; Hervé et al., 2014) (Fig. 6E).

Irrespective of temporal  $\delta^{18}\text{O}$  trends, O isotopes are useful to evaluate the possibility of crustal material (e.g., underthrust or subducted) in the source region during flare ups. Studies of tilted crustal sections indicate that the deepest, and generally least differentiated, arc rocks have  $\delta^{18}\text{O}$  values higher than mantle values. Whole rock  $\delta^{18}\text{O}$  from the deep crust in the tilted Famatinian arc is 8–9‰ (Alasino et al., 2020) and zircon  $\delta^{18}\text{O}$  from deep arc crust in the southern Sierra Nevada is 7–9‰ (Lackey et al., 2005). Elevated  $\delta^{18}\text{O}$  values in the deepest and least chemically evolved part of the crust suggest that the arc rocks acquired their isotopic values in the mantle source region, which was interpreted to primarily be (meta)sediment-contaminated lithospheric mantle in studies of the tilted arc sections (Alasino et al., 2020; Lackey et al., 2005). Pyroxenite (arclogite) xenoliths from the Sierra Nevada sample an even deeper part of the arc system (ca. 40–70 km), the residual arc root, and have reconstructed whole rock  $\delta^{18}\text{O}$  values of 6.5–8.5‰ (Ducea, 2002; Lackey et al., 2005). Garnet peridotite xenoliths from the deepest parts of the Sierra Nevada arc root (90–105 Ma) have mantle-like, reconstructed whole rock  $\delta^{18}\text{O}$  values of 5–6‰ (Chin et al., 2014). Combining data from the tilted crustal section and mantle xenoliths from the Sierra Nevada shows how  $\delta^{18}\text{O}$  varies throughout the arc column (Fig. 7). The low  $\delta^{18}\text{O}$  values for the deepest parts of the Sierra Nevada arc system suggest that the introduction of high  $\delta^{18}\text{O}$  material did not come from the slab (e.g., subducted sediments, sediment diapirs/melts). It is important to keep in mind that constraints on the  $\delta^{18}\text{O}$  composition of Sierran mantle lithosphere come from a relatively small number of samples from geographically restricted areas (e.g., Big Creek locality) within the central Sierra Nevada where the garnet peridotite xenoliths were collected (Chin et al., 2012, 2014). Along-strike increases in zircon  $\delta^{18}\text{O}$  in the southern Sierra Nevada and Mojave region have been associated with sediment subduction (Chapman et al., 2013) and an isotopically stratified lithosphere may not be universally present. Other possibilities for introducing upper crustal material with high  $\delta^{18}\text{O}$  into the upper mantle/arc root include underthrusting from the back-arc (retroarc) side (e.g., DeCelles et al., 2009), underthrusting from the forearc side (Ducea and Chapman, 2018), and downward flow within the arc (e.g., Cao et al., 2016; Paterson and

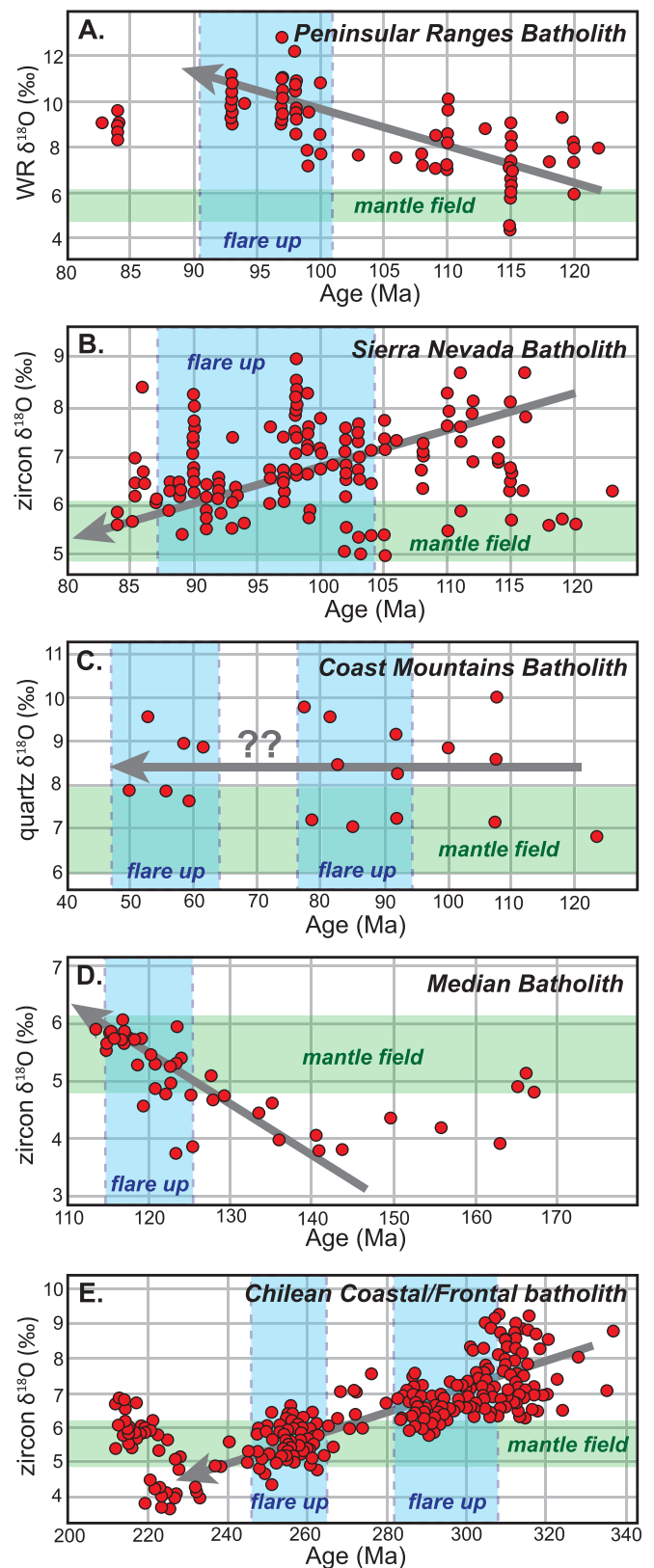


**Fig. 6.** Temporal trends in oxygen isotope ratios (red circles) exhibit a variety of patterns during arc flare ups (blue shading). A) Peninsular Ranges batholith (modified from Kistler et al., 2014; Paterson et al., 2017a, 2017b). B) Sierra Nevada batholith (modified from Lackey et al., 2008; Kirsch et al., 2016). C) Central Coast Mountains batholith (modified from Wetmore and Ducea, 2011; Cecil et al., 2018). D) Chilean Coastal and Frontal batholiths (modified from Hervé et al., 2014; del Rey et al., 2016).

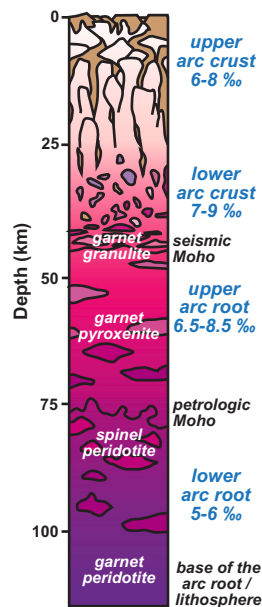


**Fig. 7.** Schematic cross section through the Sierra Nevada arc system showing how oxygen isotopic compositions vary with depth (modified from Saleeby et al., 2003). Crustal values are zircon  $\delta^{18}\text{O}$  from the southern Sierra Nevada and arc root values are reconstructed whole rock  $\delta^{18}\text{O}$  for pyroxenite to peridotite xenoliths from the central Sierra Nevada (Ducea, 2002; Lackey et al., 2005; Chin et al., 2014). Relatively low zircon  $\delta^{18}\text{O}$  in the upper arc crust in the southern Sierra Nevada was interpreted by Lackey et al. (2005) to reflect assimilation of juvenile oceanic host rocks.

Farris, 2008; Saleeby, 1990).

## 5. Geochemistry and melt fertility

There are relatively few bulk rock geochemical trends consistently observed in arc rocks during flare ups. The most commonly cited trends are increases in Sr/Y and La/Yb, which has been interpreted to reflect an increase in crustal thickness (Haschke et al., 2002a, 2002b; Girardi et al., 2012; Ducea et al., 2015a, 2015b; Profeta et al., 2015; Kirsch et al., 2016; Decker et al., 2017). Studies that relate Sr/Y and La/Yb to crustal thickness (e.g., Chapman et al., 2015; Profeta et al., 2015) focus on crystal fractionation at high pressure, which favors the crystallization of amphibole and garnet (removing HREE+Y from the melt) and suppresses plagioclase crystallization, resulting in elevated Sr (Ridolfi et al., 2010; Farmer and Lee, 2017; Ducea et al., 2020a). Where geochemical indicators of crustal thickening are apparent, they are supported by patterns of intra-arc strain and from mass balance calculations (Cao et al., 2015; Cao et al., 2016).

However, temporal trends in Sr/Y and La/Yb in many arcs do not correlate neatly with flare up events and may be interpreted in multiple ways. For example, crustal thickness doubled during the Cretaceous Sierra Nevada flare up (Profeta et al., 2015; Cao et al., 2016), but the earlier Jurassic and Triassic flare ups in the Sierra Nevada batholith record lower La/Yb values and lack prominent changes in REE ratios (Fig. 8). Deposition of marine sediments in the Sierra Nevada has also been interpreted to reflect thinner crust during the Jurassic flare up, assuming isostatically supported elevation (Cao et al., 2015).

Spatial and temporal trends of decreasing Dy/Yb have been recognized during the landward migration and flare up in the Cretaceous Sierra Nevada (Ardill et al., 2018). Decreasing Dy/Yb in arc rocks during flare ups suggests that amphibole, rather than garnet, is the most important early crystallizing phase for most arcs (e.g., Davidson et al., 2007). However, Dy/Yb progressively increases across multiple flare up events (Fig. 8A). Whether this signal is spatially or temporally controlled

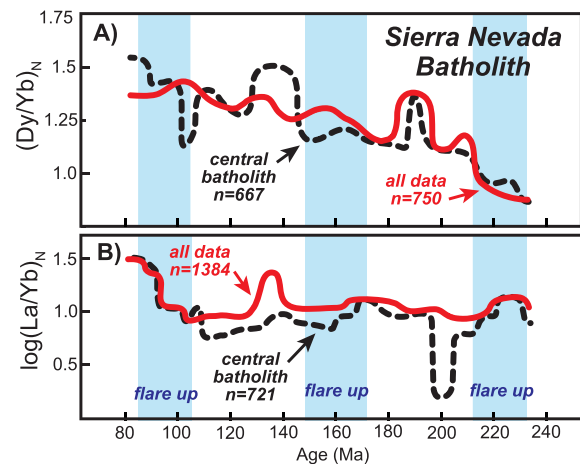


**Fig. 8.** Summary of  $(\text{Dy}/\text{Yb})_N$  (panel A) and  $\log(\text{La}/\text{Yb})_N$  (panel B) ratios for Sierra Nevada arc rocks. Plots show running medians of bivariate kernel density estimates (Sundell et al., 2019). Sierra Nevada-wide data (solid red line) from Kirsch et al. (2016, and references therein) is compared to data from only the central Sierra Nevada batholith (dashed black line), from Ardill (2020, and references therein). Rare earth element ratios are normalized to chondrite composition of Anders and Grevesse (1989).

at the arc scale remains an important question to study. Another way to stabilize amphibole  $\pm$  garnet and to suppress plagioclase crystallization is to increase water content in a melt (Müntener et al., 2001). Water saturation increases with pressure so that the role of water versus crustal thickness in producing Sr/Y and La/Yb trends cannot be completely separated (Baker and Alletti, 2012). Chapman and Ducea (2019) hypothesized that increases in La/Yb, Sr/Y, and oxygen fugacity during the Late Cretaceous flare up in the Sierra Nevada batholith could be related to partial melting of fluid-metasomatized portions of the mantle lithosphere.

Lithospheric mantle metasomatism may take the form of stalled basaltic magmas (e.g., clinopyroxene- and orthopyroxene-rich pyroxenite veins), crystallization of hydrous minerals (e.g., phlogopite), increasingly hydrated nominally anhydrous minerals (e.g., olivine, pyroxene, garnet), and hydrous silicate melts from the slab (e.g., slab and sediment melt). Storage and accumulation of these metasomatic products refertilizes the mantle lithosphere, increasing its melt-fertility (O'Reilly and Griffin, 2013). Mantle lithosphere xenoliths from the Sierra Nevada exhibit evidence for modal metasomatism (Chin et al., 2012, 2014; Ducea and Saleeby, 1996; Lee, 2005) and contain veins of garnet websterites (Ducea et al., 2020a), representing stalled mafic magmas that are demonstrably older (by ca. 40 Myr) than the arclogites of the MASH zone (Ducea and Saleeby, 1998). Similarly, exhumed continental mantle lithosphere from beneath the Median batholith in southwest New Zealand, the “Anita peridotite,” shows evidence for extensive metasomatic enrichment consisting chiefly of clinopyroxene-plagioclase aggregates that reacted with hydrous fluids to form amphibole (Czertowicz et al., 2016). The timing of enrichment of the Anita peridotite is estimated to have occurred between 100 and 250 Ma, an age range that includes the Median batholith flare up at  $\sim$ 120 Ma (Czertowicz et al., 2016; Schwartz et al., 2017). The metasomatic enrichment of the mantle lithosphere in these examples was interpreted to be caused by infiltration of hydrous basaltic melts originating in the asthenospheric mantle wedge (Chin et al., 2014; Czertowicz et al., 2016). Evidence for subduction-related, metasomatic melt-rock interactions in the mantle lithosphere beneath continental arcs is widespread and has been interpreted to be related to asthenosphere-derived melts (e.g., Canadian Cordillera, Peslier et al., 2002; Korean arc, Whattam et al., 2011) and slab-derived melts (e.g., Trans-Mexican arc, Blatter and Carmichael, 1998; Kamchatka arc, Halama et al., 2009).

Metasomatism of the mantle lithosphere via the addition of sediment-derived fluids and/or melts is also common, which is commonly thought to be associated with *syn*-collisional, high-K magmatism (e.g., Tibet; Turner et al., 1996; Anatolia, Ersoy et al., 2010). Irrespective of the type of metasomatism, melting of refertilized mantle lithosphere can contribute to asthenospheric mantle melt production and could help explain increased magma production during flare up events. Lithospheric mantle sources are expected to be exhausted relatively quickly (e.g., Harry and Leeman, 1995), which may also help explain the limited duration of many flare ups. Volumes and rates of melt produced from the asthenospheric and lithospheric mantle are discussed below in Sections 7 and 8.

Refertilization of previously melt-depleted mantle lithosphere can cause it to become even more melt-fertile than asthenospheric mantle wedge peridotite (Lambart et al., 2012, 2016). To demonstrate the melt-fertility of metasomatized mantle lithosphere we used pMELTS (Ghiorso et al., 2002) to model hydrous partial melting of refertilized lithospheric mantle (Fig. 9). For our starting composition, we used a lithospheric mantle xenolith from the central Sierra Nevada (Big Creek locality) that was refertilized by the addition of asthenospheric mantle-derived melts (Chin et al., 2012, 2014; Lee, 2005). We conservatively assumed 2 wt% H<sub>2</sub>O in the starting composition, which is consistent with water content expelled from the deepest (ca. 125–150 km depth), hottest parts of a dehydrating slab (Schmidt and Poli, 1998; Grove et al., 2012). Seismic studies estimate that water contents in shallower parts (ca. 50–125 km depth) of the mantle wedge are 3–6 wt% (Carlson and Miller, 2003). We calculated melt fractions at 1–3 GPa and temperatures up to 1400 °C (Fig. 9), which is intended to represent a ~ 60 km thick mantle lithosphere layer located beneath continental crust of normal thickness (30–40 km) and the thermal structure of the mantle wedge (e.g., Schmidt and Poli, 1998). The pMELTS modeling suggests 15–30% melt in the deep lithosphere (2–3 GPa, 1300–1400 °C), which is about twice as large as melt fractions predicted for hydrous melting of the asthenospheric mantle wedge at similar temperature and pressure conditions (e.g., 5–15%; Grove et al., 2012). Chin et al. (2014) estimated that the lithospheric mantle beneath the Sierra Nevada was refertilized by up to 30% basaltic additions, which makes the high melt fractions unremarkable – these metasomatic additions will readily melt once they

are subjected to mantle wedge temperatures.

Besides asthenospheric mantle-derived basaltic melt (e.g., garnet websterite), hydrous silicate slab-melts or sediment-melts may refertilize the mantle lithosphere. An experimental melting study by Lara and Dasgupta (2020) produced ~20% melt from a peridotite + slab-melt mixture at 2–3 GPa, 1250 °C, and with 3.5 wt% H<sub>2</sub>O. Experimental melting studies of peridotite + sediment-melt at 2–3 GPa, 1150–1300 °C, and with 2–4 wt% H<sub>2</sub>O generated 25–35% melt (Mallik et al., 2015, 2016; Grove and Till, 2019). Similar peridotite + sediment-melt experiments at lower pressures (1.5–2 GPa) yielded higher melt percentages, up to ca. 45% (Mitchell and Grove, 2015). Regardless of the exact metasomatic agent (e.g., saline and CO<sub>2</sub> fluids can be important in some cases; Newton and Manning, 2010), these experiments suggest that melting of refertilized continental mantle lithosphere can contribute a significant amount of melt to arc systems and, when combined with asthenosphere-derived melt volumes, can help explain the enormous amounts of magma generated during flare ups.

## 6. Arc crust production rates

Arc crust production refers to all igneous arc rocks, regardless of their derivation from the mantle or pre-existing crust. Average arc crust production rates during flare ups are 70–90 km<sup>3</sup> km<sup>-1</sup> Myr<sup>-1</sup> compared to <20 km<sup>3</sup> km<sup>-1</sup> Myr<sup>-1</sup> during magmatic lulls (Ducea et al., 2015a, 2015b; Paterson and Ducea, 2015; Ratschbacher et al., 2019). Detailed studies of individual intrusive suites that formed during flare ups indicate rapid construction (<5 Myr) and high arc crust production rates of 250–400 km<sup>3</sup> km<sup>-1</sup> Myr<sup>-1</sup> (Ducea et al., 2017; Klein et al., 2021; Otamendi et al., 2020). By comparison, recent estimates for crust production rates in island arcs are generally 30–90 km<sup>3</sup> km<sup>-1</sup> Myr<sup>-1</sup> (Dimalanta et al., 2002; Jicha and Jagoutz, 2015; Ratschbacher et al., 2019), which were revised upward from previous estimates (Crisp, 1984; Reymer and Schubert, 1984).

The average arc crust production rate during flare ups in continental arcs is similar to, or marginally higher than, long-term arc crust production rates from ocean island arcs that do not involve continental lithosphere or exhibit flare ups. This suggests that flare ups are not the only “abnormal” arc activity; magmatic lulls may be equally anomalous (Jicha and Jagoutz, 2015). Models attempting to explain episodic to periodic behavior in Cordilleran orogenic systems have generally sought to explain the causes of flare ups, but new models are needed to also explain suppressed arc crust production (i.e., magmatic additions to the crust) during magmatic lulls. We propose that accumulation of mantle-derived melts and slab-derived fluids in the mantle lithosphere is a viable mechanism to suppress the delivery of magmas to the arc during magmatic lulls and account for the voluminous magmatic additions during flare ups. This metasomatic accumulation may take place immediately outside of melt-pathways (i.e., the active magmatic “plumbing system”) beneath the arc, including in the back-arc. Subsequent melting of this metasomatized lithosphere can add to background levels of asthenosphere-derived melt and can explain higher crustal production rates during flare ups (Chapman and Ducea, 2019). In this hypothesis, the mantle lithosphere acts as a temporary storage container for some mantle-derived melt products (e.g., clinopyroxene-rich dikes).

## 7. Mantle-derived melt production rates

It is instructive to compare arc crust production rates to melt production estimates from the mantle wedge beneath the arc, referred to as mantle-derived melt production rates. This entity is different from mantle addition rates to the crust because it is concerned with the amount of melt produced in the mantle wedge, rather than the preservation of that melt/magma as part of the crust (Table 1).

The chemical composition of both intraoceanic island arcs and continental arcs cannot be directly produced by melting the upper mantle and requires additional processes like fractionation and partial

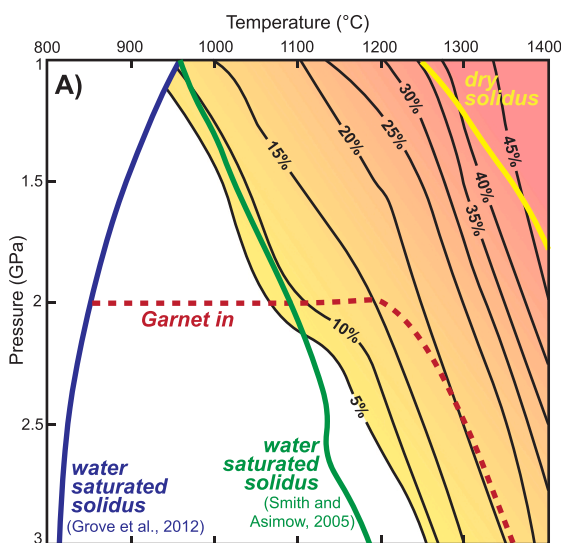


**Fig. 9.** Phase diagram for a clinopyroxene-rich (~20% mode) garnet-bearing spinel peridotite xenolith from the central Sierra Nevada (sample 1026 V; Lee, 2005; Chin et al., 2012, 2014) that represents part of the deep (ca. 3 GPa) mantle lithosphere that was metasomatized by the addition of asthenosphere mantle-derived melts. Melt fractions and garnet stability were calculated with pMELTS (Ghiorso et al., 2002; Smith and Asimow, 2005) at  $\Delta FMQ = -1$  with 2 wt% added water.

melting of basaltic rocks that will generate large mafic to ultramafic residues consisting of restite and cumulate assemblages (Ducea, 2002; Jagoutz, 2014). Continental arcs experience magmatic and tectonic thickening during flare ups (Cao et al., 2015) and the residual assemblages to felsic batholith rocks can be an eclogite facies rock, named arclogite in thick arcs, that can founder or delaminate into the mantle and help explain the intermediate composition of continental crust created at arcs (Ducea et al., 2020a; 2020b). Arclogite and arc roots that have delaminated into the mantle are not included in long-term arc crust production rates (e.g., Ratschbacher et al., 2019), but represent a substantial crustal volume that needs to be accounted for in order to calculate mantle-derived melt production rates. The ratio of arclogite/residual assemblages to felsic arc crust is approximately 2:1 (Ducea, 2002; Jagoutz and Schmidt, 2013). The amount of arc material lost to delamination can be estimated based on chemical and mass-balance calculations when information is available on the composition of the deep arc crust, usually obtained from seismic studies or tilted crustal sections (Ducea, 2002; Saleeby et al., 2003; Lee et al., 2006; Jagoutz and Schmidt, 2013). Long-term estimates (across flare ups and lulls) for the flux of arc roots into the mantle from both intraoceanic arcs and continental arcs are 10–100 km<sup>3</sup> km<sup>-1</sup> Myr<sup>-1</sup> (Ducea et al., 2015a; Jagoutz and Kelemen, 2015). For example, Ducea (2002) suggested a long-term rate of 25–40 km<sup>3</sup> km<sup>-1</sup> Myr<sup>-1</sup> for the Sierra Nevada batholith.

Arclogitic arc roots are chiefly produced during arc flare up events (Ducea, 2001) and the volume of delaminated arc roots can be added to arc crust production rates and combined with models for the degree of (pre-existing) crustal assimilation to estimate mantle-derived melt production rate. The ratio of crustal to mantle contributions for preserved arc crust is up to 1:1 for continental arcs (Lackey et al., 2005; Kay et al., 2010; Ducea et al., 2015a, 2015b; Freymuth et al., 2015; Schwartz et al., *in press*). Stable isotope studies indicate that arclogites also contain a crustal component and Ducea et al. (2020a) suggested that the entire arclogite-batholith system in continental arcs contains at least 15–25% of recycled lower crustal material. Assuming a 2:1 arclogite to felsic crust ratio, 20% recycling of preexisting crustal material, and average flare up arc crust production rates of 70–90 km<sup>3</sup> km<sup>-1</sup> Myr<sup>-1</sup>, the mantle-derived melt production rate for continental arcs during flare ups is 170–215 km<sup>3</sup> km<sup>-1</sup> Myr<sup>-1</sup>. The same calculation with a 1.5:1 arclogite to felsic crust ratio suggests mantle-derived melt production rates of 140–180 km<sup>3</sup> km<sup>-1</sup> Myr<sup>-1</sup>. These values compare favorably to mantle-derived melt production rates for intraoceanic island arcs (160–290 km<sup>3</sup> km<sup>-1</sup> Myr<sup>-1</sup>) that exhibit limited crustal assimilation (Jicha et al., 2006; Jicha and Jagoutz, 2015; Ratschbacher et al., 2019). Klein et al. (2021) recently performed similar calculations for the Bear Valley intrusive suite in the Sierra Nevada batholith and suggested that the mantle-derived melt production rate was >750 km<sup>3</sup> km<sup>-1</sup> Myr<sup>-1</sup>, which may be the highest rate ever reported for subduction-related magmatism.

Continental arcs that have not experienced delamination would preserve thicker sections of mafic lower crust and yield higher estimates of mantle-derived melt production. For example, it is unclear if the relatively thin (~30 km) Famatinian arc experienced delamination because it preserves ~15 km of mafic lower crust complementary to the felsic upper crust (Otamendi et al., 2012). Even without the loss of an arc root, however, the Famatinian arc is estimated to have had a maximum mantle-derived melt production rate of ~180 km<sup>3</sup> km<sup>-1</sup> Myr<sup>-1</sup> and an average mantle-derived melt production rate of ~125 km<sup>3</sup> km<sup>-1</sup> Myr<sup>-1</sup> during the Ordovician flare up (Ducea et al., 2017; Otamendi et al., 2020). Setting aside the high estimate of Klein et al. (2021) that focused on a single intrusive suite, the range of mantle-derived melt production rates during flare ups in convergent continental arcs is 140–215 km<sup>3</sup> km<sup>-1</sup> Myr<sup>-1</sup>. Mantle-derived melt production rates for continental arcs during magmatic lulls are ≤15 km<sup>3</sup> km<sup>-1</sup> Myr<sup>-1</sup> assuming limited arc root production (1:1 residual assemblage to felsic crust ratio) and 20% recycling of crust for the arc root-batholith system. Crustal assimilation and the development of arc roots is thought to be less efficient during

magmatic lulls (Ducea, 2001; Ducea and Barton, 2007). To get a sense of what these rates imply for long-term mantle-derived melt production, consider a 60 Myr periodic pattern with 10 Myr-long flare ups with production rates of 180 km<sup>3</sup> km<sup>-1</sup> Myr<sup>-1</sup> and 50 Myr-long lulls with 10 km<sup>3</sup> km<sup>-1</sup> Myr<sup>-1</sup> production rates. The long-term mantle-derived melt production rate would be 40 km<sup>3</sup> km<sup>-1</sup> Myr<sup>-1</sup>. Extending the duration of flare ups and shortening the duration of magmatic lulls will increase this rate. As an end-member example, if we perform the same hypothetical calculation as above, but assume that flare ups and lulls have the same duration (30 Myr each in the 60 Myr cycle example), the long-term mantle-derived melt production rate is 95 km<sup>3</sup> km<sup>-1</sup> Myr<sup>-1</sup>.

How do our calculated mantle-derived melt production rates compare to other independent estimates of melt production from the mantle wedge? Numerical models of subduction zones that are coupled to mantle melting models (e.g., Katz et al., 2003; Kelley et al., 2010; Portnyagin et al., 2007) suggest mantle-derived melt production rates of 10–70 km<sup>3</sup> km<sup>-1</sup> Myr<sup>-1</sup> (Cagnioncle et al., 2007; Cerpa et al., 2019; Gerya and Meilick, 2011; Hebert et al., 2009; Vogt et al., 2012; Zhu et al., 2013). Mantle-derived melt production rates based on water outgassing and the water content in primary magmas range from ~30 km<sup>3</sup> km<sup>-1</sup> Myr<sup>-1</sup> for individual arcs (e.g., Cascade arc; Ruscitto et al., 2012) to 125 km<sup>3</sup> km<sup>-1</sup> Myr<sup>-1</sup> based on global averages (Bekaert et al., 2020). Mantle-derived melt production rates calculated using regional heat flow data are 10–35 km<sup>3</sup> km<sup>-1</sup> Myr<sup>-1</sup> (Ingebritsen et al., 1989; Guffani et al., 1996; Manga et al., 2012). Mantle-derived melt production rates <50 km<sup>3</sup> km<sup>-1</sup> Myr<sup>-1</sup> have also been estimated by modeling the enthalpy of mantle-derived intrusions required to match a given amount of crustal assimilation (Grunder, 1995). These independent estimates suggest that melt production rates from the mantle wedge are ≤125 km<sup>3</sup> km<sup>-1</sup> Myr<sup>-1</sup>, and mainly 10–70 km<sup>3</sup> km<sup>-1</sup> Myr<sup>-1</sup>, which is similar to the range of estimates for long-term mantle-derived melt production rate in our hypothetical 60 Myr example (40–95 km<sup>3</sup> km<sup>-1</sup> Myr<sup>-1</sup>).

It is important to keep in mind that these rates are not new continental crust production rates. Assuming a 1:1 ratio of mantle to crustal sources for new arc crust and considering the same hypothetical 60 Myr-long example (10 Myr-long flare ups, 50 Myr-long lulls), the long-term production rate for generating new continental crust is 9–16 km<sup>3</sup> km<sup>-1</sup> Myr<sup>-1</sup>, based on our estimates of arc crust production rates discussed in Section 6. This matches the long-term estimates for growth of continental crust since ~3 Ga (0.6–0.9 km<sup>3</sup>/yr; Hawkesworth et al., 2019), which is 11–16 km<sup>3</sup> km<sup>-1</sup> Myr<sup>-1</sup> spread out over the modern total length of trenches (55,000 km).

## 8. Variable melting in the mantle wedge

Considering flare ups in terms of melt production in the mantle wedge is useful because melt fraction or melt volume is an output of some numerical and petrologic models of subduction zones. There are a variety of ways that changes in subduction parameters could influence melt production in the mantle wedge including changes in temperature, water flux, slab dip, and mantle convection. These parameters are all interrelated and often associated with changes in convergence rate. An increase in plate convergence rate has been proposed to increase the degree and amount of melt produced in subduction zones (e.g., England and Katz, 2010; Turner and Langmuir, 2015a, 2015b) and may be a possible trigger for flare ups in Cordilleran systems (e.g., Hughes and Mahood, 2008). There are two reasons why changes in plate convergence rate are unlikely to trigger flare ups. First, there is either no correlation or a poor correlation between the timing of flare ups and changes in plate motion and convergence rate (Cao et al., 2016; DeCelles et al., 2009; Ducea, 2001; Ducea et al., 2020b; Kirsch et al., 2016; Zhang et al., 2019b). This correlation can be improved if variable “lag times” are added, but the duration of these lag times and the physical processes they represent are not well constrained (e.g., Kirsch et al., 2016). Among the many possibilities, lag times could represent incubation periods in

the deep crust or the time it takes the arc system to respond to tectonic perturbations (see Section 9 below). Second, the magnitude of the increase in melt production required to match the difference between magmatic lulls and flare ups (ca. 100–200 km<sup>3</sup> km<sup>-1</sup> Myr<sup>-1</sup>), is outside the range of modeled values.

Cagnioncle et al. (2007) modeled melt production rate in the mantle wedge as a function of convergence rate and observed a linear increase of 2 km<sup>3</sup> km<sup>-1</sup> Myr<sup>-1</sup> for every 10 mm/yr increase in convergence rate (Fig. 10). Zhu et al. (2013) performed similar modeling and observed a ~ 5 km<sup>3</sup> km<sup>-1</sup> Myr<sup>-1</sup> increase in mantle melt production for a 10 mm/yr increase in convergence rate. These models incorporated both fluid-flux melting and decompression/dehydration melting in the mantle wedge and explored the effects of increases in mantle hydration, temperature, and availability of melt-fertile mantle rocks as a result of increased convergence rate. Most continental arcs experience changes in convergence rate throughout their lifetime, but they generally do not experience the extreme variations needed to produce a flare up predicted by the modeling studies. For example, for the Sierra Nevada batholith, Farallon-North American convergence rates were 50–90 mm/yr during the mid-Cretaceous magmatic lull and were 60–100 mm/yr during the Late Cretaceous flare up (Torsvik et al., 2019). Using the most extreme estimates, this suggests that ca. 25 km<sup>3</sup> km<sup>-1</sup> Myr<sup>-1</sup> more mantle-derived melt was produced during the Late Cretaceous flare-up as a result of increased convergence rates. This is too low to explain the differences observed in the Sierra Nevada batholith (Fig. 10). If the modeling results are applicable to arcs globally, it suggests that subduction parameters related to increasing convergence rate (e.g., temperature, water flux, mantle convection, etc.) are not what drives flare ups and lulls in convergent Cordilleran orogenic systems. Another way to state this is that the difference in mantle-derived melt production between flare ups and lulls cannot be explained by variations within the range of subduction parameters considered “normal” (i.e., the global range of observed values) according to existing models. Something extraordinary must occur.

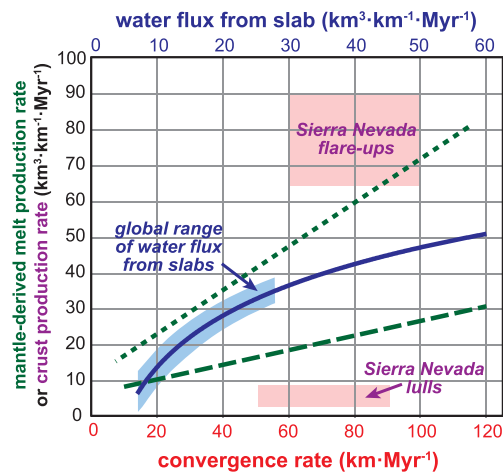


**Fig. 10.** Numerical modeling studies by Cagnioncle et al. (2007) (long-dashed green line) and Zhu et al. (2013) (short-dashed green line) showed that mantle-derived melt production rate from the mantle wedge varies linearly as a function of convergence rate (lower x-axis). Based on this modeling, the difference in the Farallon-North America convergence rate between the mid-Cretaceous flare up and the Early Cretaceous magmatic lull (pink shaded areas) is too small to account for difference in crust production rate (plotted on the same y-axis scale as mantle-derived melt production rate). Plate convergence rates are from Torsvik et al. (2008; 2019) and Sierra Nevada data are from Ducea et al. (2015a, 2015b). Cagnioncle et al. (2007) also modeled how increasing water flux from the subducting plate (solid blue line; upper x-axis) affects mantle-derived melt production rate in the mantle wedge. The global range of water released from slabs up to 200 km depth is shown by the blue shaded area (van Keken et al., 2011).

Water flux from the slab is a good example to illustrate this point. Additional water, or volatiles more broadly, released from the slab will increase melting of the mantle wedge (Grove et al., 2006; Ulmer, 2001) and could potentially spark flare ups in continental arcs. The global range of water flux released from slabs to 200 km depth in subduction zones is 6–28 Tg Myr<sup>-1</sup> m<sup>-1</sup> (van Keken et al., 2011). Assuming a water density of 1000 kg/m<sup>3</sup> and ignoring density variations associated with changing pressure and temperature conditions, this is equivalent to a volumetric flux (6–28 km<sup>3</sup> km<sup>-1</sup> Myr<sup>-1</sup>). The modeling results of Cagnioncle et al. (2007) suggests that the difference in melt production from the mantle wedge over the global range of slab water flux is ca. 30 km<sup>3</sup> km<sup>-1</sup> Myr<sup>-1</sup>, which is too low to explain the differences between flare ups and lulls in continental arcs (Fig. 10). If increased water content in the mantle wedge is the cause of a flare up, then that water must be supplied in addition to what is considered within the normal range of water released from the slab.

Results of numerical modeling studies should always be viewed with an open mind, but the principal issue with relating these studies to flare ups is that the amount of magma added to arc systems during major flare ups is so massive that it violates what modeling studies have considered to be realistic scenarios involving melting of the mantle wedge. Numerical studies generally do not predict mantle-derived melt production rates >100 km<sup>3</sup> km<sup>-1</sup> Myr<sup>-1</sup> under “normal” subduction parameters unless it involves back-arc spreading and the formation of new oceanic crust (Gerya and Meilick, 2011; Nikolaeva et al., 2008; Vogt et al., 2012; Zhu et al., 2019). Although fluctuating subduction parameters like convergence rate appear to be unlikely to explain the difference in melt production between flare ups and lulls, there are many out-of-the-ordinary mechanisms to increase melting in the upper mantle and deep lithosphere including processes like slab break-off (e.g., Schwartz et al., 2017, in press), subduction of hydrated fracture zones (e.g., Manea et al., 2014), or subduction of serpentinized continental mantle lithosphere preceding continental collision (e.g., Ganade et al., 2021). These types of processes can explain individual flare up events, but struggle to explain episodic alternations between magmatic lulls and flare ups.

Another explanation for high mantle-derived melt production rates is that melt is being generated from the mantle lithosphere in addition to the asthenospheric mantle wedge (Chapman and Ducea, 2019). Contributions from (refertilized) mantle lithosphere are generally not included in numerical studies but could help to explain melt production discrepancies and obviates the need to find extraordinary processes for melting in the asthenospheric mantle wedge. For example, assuming a 50 km<sup>2</sup> mantle lithosphere-melt source region beneath a continental arc and 20% melting (e.g., Fig. 3), 500 km<sup>3</sup> km<sup>-1</sup> of mantle-derived melt will be generated, or 100 km<sup>3</sup> km<sup>-1</sup> Myr<sup>-1</sup> distributed over a 5 Myr long flare up event. Unlike the convecting asthenospheric mantle, melt contributions from the lithospheric mantle are not replenished unless mantle lithosphere is underthrust into the arc.

The mid-Cenozoic ignimbrite flare up in the western U.S. Cordillera was not confined to the frontal arc, but it may be a useful analog when considering melt production from the mantle lithosphere. The Farallon plate is believed to have hydrated, refertilized, and refrigerated the Proterozoic North American mantle lithosphere during low-angle subduction as part of the Laramide Orogeny (ca. 80–40 Ma) (Humphreys et al., 2003). During the middle Cenozoic, the Farallon slab rolled back or foundered and exposed the metasomatized mantle lithosphere to upwelling sub-lithospheric mantle that heated the lithosphere and produced voluminous magmatism, including the Mogollon-Datil and San Juan volcanic fields (Davis and Hawkesworth, 1993; Lipman, 1992). Using magmatic volumes and isotopic compositions, Farmer et al. (2008) estimated lithospheric mantle-derived melt volumes of 2 M km<sup>3</sup> for the Mogollon-Datil field and 7 M km<sup>3</sup> for the San Juan field. Based on the range of igneous rock ages in these fields and the possible radii of the of lithospheric mantle source regions surrounding the fields, reported by Farmer et al. (2008), these values indicate mantle-derived melt

production rates of  $\sim 1150 \text{ km}^3 \text{ km}^{-1} \text{ Myr}^{-1}$  for the San Juan volcanic field and  $\sim 650 \text{ km}^3 \text{ km}^{-1} \text{ Myr}^{-1}$  for the Mogollon Datil volcanic field. Only a fraction of these estimates is enough to explain the relatively high mantle-derived melt production rates during flare ups in continental arcs. The key factors in producing the mid-Cenozoic ignimbrite flare up, and plausibly continental arc flare ups as well, are metasomatic refertilization of the mantle lithosphere and added heat from the mantle to melt the refertilized mantle. The source of the heat in the mid-Cenozoic ignimbrite flare up model is upwelling asthenosphere (Farmer et al., 2008; Humphreys et al., 2003) whereas added heat may arise from other factors in continental arc systems, including migration of the arc and attendant mantle wedge (Chapman and Ducea, 2019).

## 9. Punctuated melt extraction

The mantle-derived melt production rates calculated above assume that there is minimal “lag time” between mantle melting and emplacement of (chiefly intermediate) arc magmas in the middle to upper crust where magmatic addition rates are often determined from. Is this a good assumption? Investigations of short-lived isotopes indicate that melt extraction from the mantle wedge is rapid, on the order of  $10^1$  kyr or less (e.g., Turner et al., 1997). Analog studies and numerical models that consider porous flow also suggest that melt migration beneath arcs is rapid, on the order of  $10^1$ – $10^2$  kyr once fluid pathways are established (e.g., Connolly et al., 2009; Wada and Behn, 2015). Numerical models of mantle wedge plumes or diapirs suggest a range of melt migration velocities, but generally predict that melt extraction occurs in  $\leq 1$  Myr (e.g., Gerya and Yuen, 2003). These studies suggest that if lag times are important for producing flare ups and lulls, that they are likely related to crustal, rather than mantle, processes. The dominant paradigm for producing intermediate to felsic arc magmas is that hydrous, mantle-derived basaltic melts intrude into a MASH (melting, assimilation, storage, homogenization) or deep crustal hot zone, mix with older intrusions and cumulates, and melt preexisting lower crustal rocks (Hildreth and Moorbath, 1988; Barboza and Bergantz, 2000; Dufek and Bergantz, 2005; Annen et al., 2006). It is possible that the episodic nature of flare ups in continental arcs is related to the time it takes for melt to be differentiated, segregated, and extracted from these deep crustal hot zones (Annen et al., 2015; Ducea et al., 2020b). This is an alternative to the model that emphasizes the role of the mantle lithosphere discussed above.

Modeling studies suggest that the intrusion of mantle-derived basaltic dikes into the lower crust will produce large volumes of intermediate magmas and residual melt at timescales of 0.1–10 Myr for a wide range of emplacement rates, intrusion geometries, dike compositions, and crustal compositions (Petford and Gallagher, 2001; Annen and Sparks, 2002; Dufek and Bergantz, 2005; Annen et al., 2006). In the modeling studies, these values represent the time between the start of mantle-derived basaltic intrusion and the creation of intermediate melt fractions large enough to be extracted. Melt extraction is thought to be controlled by a rheological transition (e.g., “solid-to-liquid transition;” Rosenberg and Handy, 2005) or melt-connectivity transition (Brown, 2007) when the melt fraction reaches a threshold (e.g., “critical melt fraction;” van der Molen and Paterson, 1979). At low strain rates, this threshold is estimated at 0.4–0.7 melt fraction (Petford, 2003; Rosenberg and Handy, 2005; Costa et al., 2009; Castruccio et al., 2010). Modeling studies using these thresholds predict that the timescale for differentiation, segregation, and extraction of melt from MASH or deep crustal hot zones is ca. 10 kyr to 1 Myr (Jackson et al., 2018; Petrelli and Zellmer, 2020; Riel et al., 2019; Solano et al., 2012). These could be considered maximum estimates for a couple of reasons. First, these estimates neglect complexities such as pressure gradients from tectonic forces, melt transport through fraction/channel networks, and melt-assisted decompaction (Sawyer, 1994; Brown et al., 1995; Rushmer and Miller, 2006; Connolly and Podladchikov, 2007). Second, some studies have suggested that the melt fraction threshold for extraction is

much lower ( $< 0.1$ ) (see review in Clemens and Stevens, 2016). Field studies of exposed deep crustal MASH zones also indicate that melt extraction is efficient (Jagoutz et al., 2006; Walker Jr et al., 2015). For example, high-precision geochronology and isotopic data from an exposed upper mantle to lower crustal section through the Kohistan arc suggest that changes in the mantle source region were reflected in crustal arc rocks in  $< 4$  Myr (Bouilhol et al., 2011), which implies melt extraction and isotopic homogenization on similar timescales.

These studies suggest that the lag time between mantle melting and emplacement of felsic arc rocks in the middle to upper crust may be  $< 10$  Myr, but these processes are still poorly understood. The Paleogene and Late Cretaceous flare ups in the southern Coast Mountains batholith coincide with a shift to higher zircon U/Th (Gehrels et al., 2009), which Ducea et al. (2020b) interpreted to reflect high-temperature metamorphism in deep arc roots. One possibility is that basaltic additions from the mantle during magmatic lulls slowly heat up and thicken the arc root (over 10s of Myr) until it reaches a depth and temperature hot enough to cross a melt fraction threshold and trigger the rapid evacuation of intermediate magmas into the middle to upper crust (Ducea et al., 2020b). In this scenario, the initiation of a flare up may depend on the time it takes to grow an arc root of sufficient size. A similar situation is possible to imagine in metasomatized mantle lithosphere where veins or pockets of partially molten pyroxenite may be surrounded by solid peridotite that prevents melt extraction at low degrees of melting (e.g., Lambart et al., 2012, 2016).

## 10. Arc migration

A compilation of arc migration patterns compared to flare up timing for several continental arcs is presented in Fig. 11. The data indicate that many flare ups coincided with landward arc migration. In these cases, landward arc migration was either concurrent with the flare up event (e.g., Median batholith, Southern Coast Mountains batholith) or began before the flare up (e.g., Korean Peninsula, Peruvian Coastal batholith; Sierra Nevada batholith). Depending on how initiation times are defined, arc migration may start up to several tens of millions of years before a corresponding flare up occurs. These patterns show that arc migration may begin during magmatic lulls and that flare ups do not occur until the arc reaches a certain distance away from the trench, which is generally 40–150 km for the examples in Fig. 11. Magmatism tends to wane, or cease, behind the landward advancing arc front. The Gangdese batholith is an exception to this pattern where only the flare-up centered at 15 Ma shows clear evidence for magmatism shutting down behind the arc front (Chapman and Kapp, 2017). Magmatism generally broadens, rather than migrates, for the Gangdese batholith flare ups centered on 93 and 50 Ma (Fig. 11G). The youngest two flare ups in the Gangdese batholith (ca. 15 and 55 Ma) occurred after India-Asia collision and have been associated with subduction of continental lithosphere and other collisional orogenic processes (see review in Kapp and DeCelles, 2019) that may not be applicable to Cordilleran continental arc systems. Regardless, most continental arcs show evidence for a broadening of the region of magmatic activity during a flare up. For example, magmatism in the Korean Peninsula was concentrated in a  $\sim 100$  km wide region (i.e., arc width) during arc migration, but that region broadened to ca. 200 km during the Jurassic flare up (Cheong and Jo, 2020), resulting in a “L” shape in the arc migration path that can be observed in many arcs (pink shaded areas in Fig. 11). Studies examining temporal changes in the radiogenic isotopic composition of arc rocks show that the range of isotope ratios can also broaden during flare ups (e.g., Ducea and Barton, 2007) (Fig. 1). Lateral changes in the age and composition of the lithosphere can explain why the range of isotopic values increases as the region of magmatic activity expands and begins to reflect melting and assimilation of more diverse lithospheric and upper mantle domains (Chapman et al., 2017).

The position of a continental arc relative to the fixed interior of the upper plate is rarely static and usually migrates at semi-continuous rates

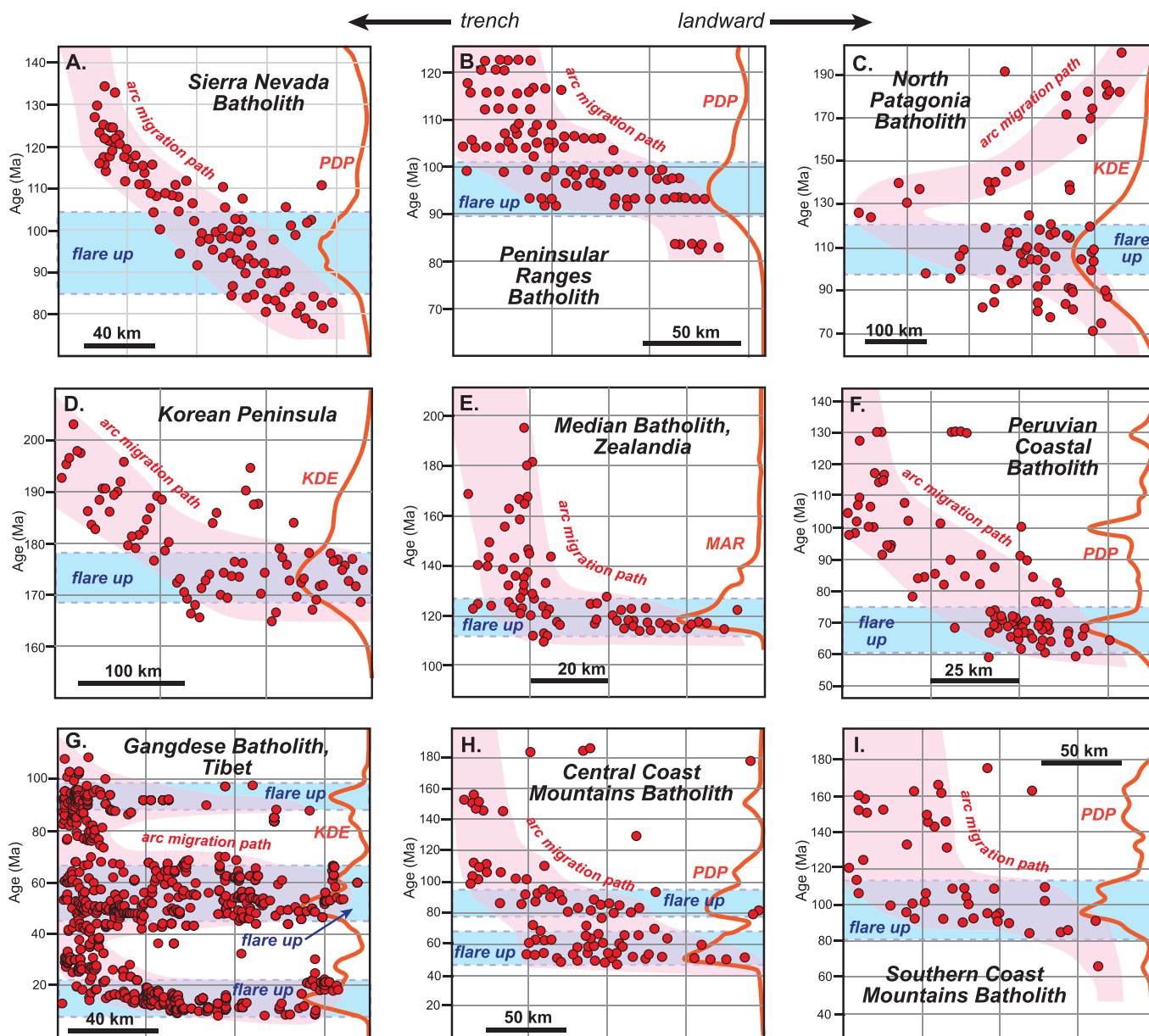


**Fig. 11.** The location of and age of magmatism (red circles) reveals arc migration patterns (pink shading) and is compared to the age of arc flare ups (blue shading), highlighted by probability density plots (PDP) of rock ages, kernel density estimates (KDE) of rock ages, or magmatic addition rates (MAR). In all panels, the distance away from the trench increases to the right. A) Sierra Nevada batholith, modified from Chapman and Ducea (2019) and Cecil et al. (2012). B) Peninsular Ranges batholith, modified from Karlstrom et al. (2014) and Paterson et al. (2017a, 2017b). C) North Patagonia batholith, generated from data compiled in Echaurren et al. (2019) along a ~ 200 km wide transect with end-points centered at 46°S/75°W and 43°S/70°W. D) Korean Peninsula arc, modified from Cheong and Jo (2020). E) Median batholith in New Zealand, modified from Schwartz et al., (2017; in press). F) Peruvian Coastal batholith, modified from Martinez-Ardila et al., 2019a, b). G) Gangdese batholith in Tibet, modified from Chapman and Kapp (2017). H) Central Coast Mountains batholith, modified from the “Terrace” transect in Cecil et al. (2018). I) Southern Coast Mountains batholith, modified from the “Vancouver” transect in Cecil et al. (2018).

of 1–5 km/Myr (Ducea et al., 2015a, 2015b). Arcs can also migrate rapidly ( $\leq 25$  km/Myr) or “jump” hundreds of kilometers landward, which is often associated with periods of ultra-shallow low-angle to flat-slab subduction (Ducea and Chapman, 2018) where subduction erosion takes an extreme form – large amounts of the forearc get subducted-accreted (underplated) to the upper plate hundreds of km inland from its original location (Ducea et al., 2009). For example, the rapid landward arc migration observed in the North Patagonia batholith (Fig. 11C) is hypothesized to be associated with a regionally extensive period of shallow subduction (Gianni et al., 2018). Steady-state arc migration is classically associated with changes in slab dip (Coney and Reynolds, 1977; Dickinson et al., 1978), but has also been linked to forearc

subduction erosion (Jicha and Kay, 2018; Kay et al., 2005). Periods of increased subduction erosion correlate to periods of shallow subduction, which makes separating these processes difficult (Ducea and Chapman, 2018; Keppie et al., 2009; Stern, 2011). Karlstrom et al. (2014) suggested that magmatic thickening of the arc (i.e., arc root growth) truncates the mantle wedge and shifts corner flow and the locus of melting away from the trench. Because continental arcs and their complementary arc roots are almost entirely constructed during flare ups (Ducea, 2001; Ducea et al., 2015a, 2015b), this model predicts that landward arc migration is driven by flare ups - the growth of the arc root during a flare up deflects the arc system landward. The data presented in Fig. 11 suggest the opposite – that landward arc migration starts before a flare

up and growth of an arc root. Truncation of the mantle wedge by growth of an arc root may contribute to extinguishing a flare up (e.g., Chin et al., 2014, 2015), but external processes like slab dynamics seem likely to control long-term or semi-steady-state arc migration.

### 11. Slab and orogen dynamics

Changes in slab dip are a common cause of arc migration and, as a result, may be important for producing arc flare ups. Specifically, decreasing slab dip (i.e., slab shallowing) will cause landward arc migration that is correlated to arc flare up events (Fig. 11). Slab shallowing is also predicted to increase plate coupling and increase upper plate deformation/shortening (e.g., Guillaume et al., 2009). This property of slab shallowing is a key component of many Cordilleran

geodynamic models including models linking flat-slab subduction to “Laramide-style” deformation (e.g., Dickinson et al., 1978; Jordan et al., 1983), accretionary orogen models that experience tectonic switching (e.g., Collins, 2002; Collins and Richards, 2008; Kemp et al., 2009), and models that relate plate coupling to forearc, hinterland, and retroarc shortening (e.g., DeCelles et al., 2009; Horton, 2018). The last type of model has been extensively applied to the Andes, where subduction angle has been proposed to control periodic alternations between contractional, neutral, and extensional tectonic regimes as well as periods of increased magmatism (DeCelles et al., 2015; Folguera and Ramos, 2011; Haschke et al., 2002a, 2002b; Horton and Fuentes, 2016; Oncken et al., 2006; Ramos, 2009). This general class of geodynamic models are often called orogenic cyclicity models because they predict that the tectonic processes repeat in a cyclical manner (e.g., Cordilleran

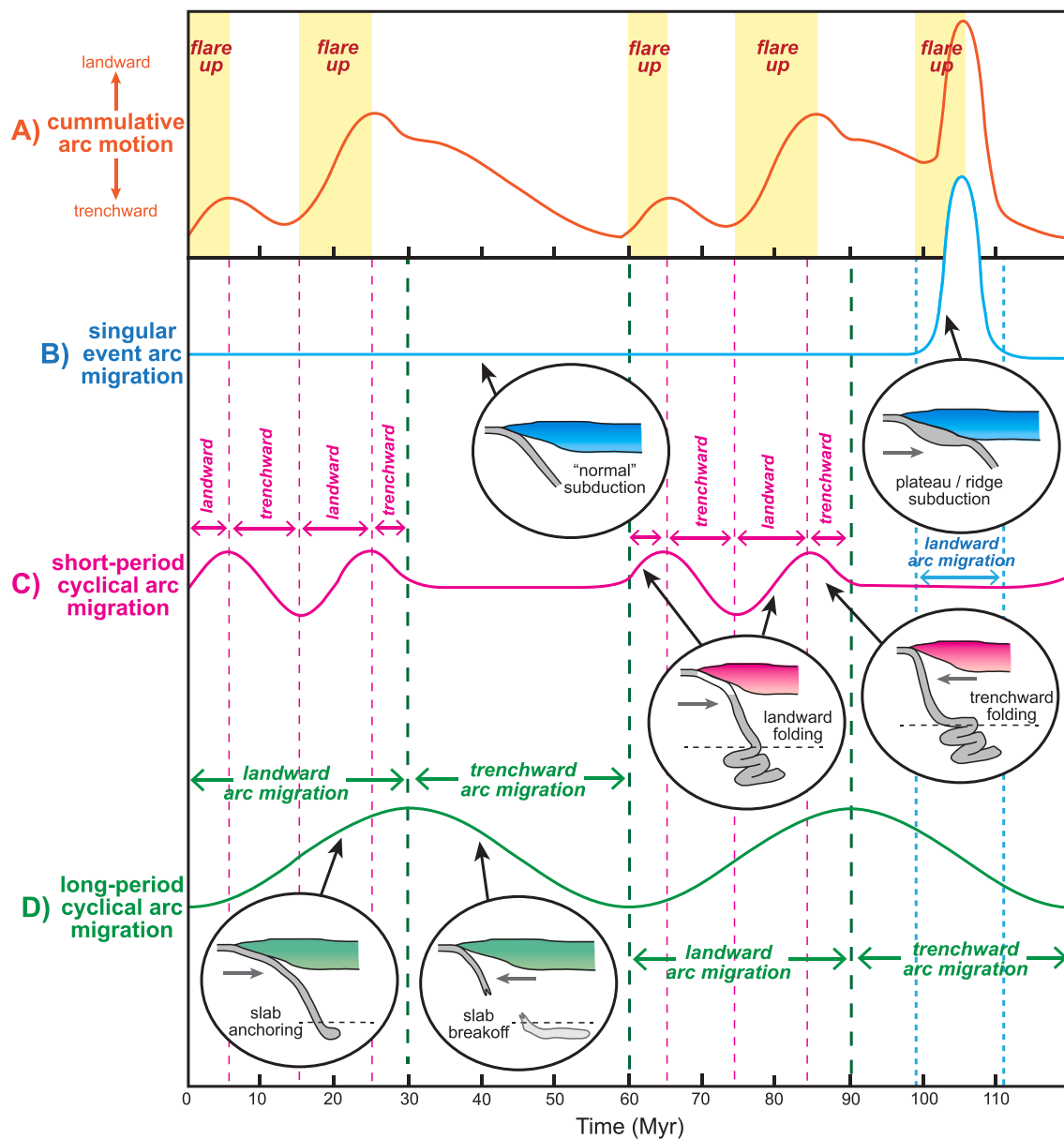


**Fig. 12.** A schematic diagram showing how multiple processes may influence slab dip and arc migration. Solid colored lines show changes in arc migration through time with landward migration directed upward and trenchward migration directed downward on the diagram. Slab anchoring and breakoff (green line) is shown as an example of a long-period (60 Myr) cyclical process. Slab folding (pink line) is shown as an example of a short-period (20 Myr) cyclical process. Slab folding is inferred to not occur when the slab is not anchored in the lower mantle (dashed black line in circular cross-sections). Subduction of an oceanic plateau or submarine ridge (blue line) is shown as an example of a “one-off” event. The cumulative effect of these processes are shown at the top of the diagram (orange line) with intervals of net landward arc migration labeled as a flare up.

cycle model, DeCelles et al., 2009; Andean orogenic cycle model, Ramos, 2009). These models all differ in detail, but the importance of periods of slab-shallowing is one unifying similarity. If arc flare up events are caused by slab shallowing and landward arc migration (e.g., Chapman and Ducea, 2019), then flare ups could be readily incorporated into, and explained by these existing orogenic cyclicity models.

There are many factors that can cause slab dip to shallow and, in terms of generating a magmatic flare up, it may not matter what the specific mechanism is (Fig. 12A). In the following section, we discuss a small subset of possible mechanisms that can produce singular, “one-off,” arc migration events (Fig. 12B), short-period cyclical arc migration (Fig. 12C), and long-period cyclical arc migration (Fig. 12D). These processes, among many others, may combine and result in a cumulative arc motion record (Fig. 12A). Interested readers are referred to Gianni and Luján (2021) for a recent, and more comprehensive, review on the myriad causes of arc migration. First, singular, “one-off,” events may cause slab shallowing. One of the most common events of this type is subduction of relatively buoyant oceanic lithosphere, including subduction of oceanic plateaus, seamount chains, and spreading ridges (Fig. 12B). Subduction of buoyant oceanic lithosphere is well-documented in many Cordilleran orogens and has been correlated with some arc flare ups (Chapman et al., 2013; Folguera and Ramos, 2011; Gianni et al., 2018; Haschke et al., 2002a, 2002b; Kay et al., 2005). Conversely, cases of extreme slab-shallowing – flat-slab subduction – are generally characterized by magmatic lulls or the complete cessation of magmatism (e.g., Pampean flat-slab segment; Ramos et al., 2002).

Some arc flare ups occur across very large segments of plate margins and require less localized processes. For example, a ~ 6000 km long segment of the Neo-Tethyan continental arc (southern Lhasa-west Burma-Sumatra) exhibits concurrent magmatic lulls and flare ups during the Cretaceous to early Paleogene, which have been attributed to repeated periods of slab steepening and shallowing (Zhang et al., 2019b). Likewise, a ~ 5000 km long segment of the western Gondwana continental arc (Patagonia-Antarctic Peninsula-Marie Byrd Land) exhibits concurrent flare ups during the mid-Cretaceous (Riley et al., 2018; Tulloch and Kimbrough, 2003) and a > 3000 km long segment of the North American Cordilleran arc (southern Coast Mountains-Sierra Nevada-Peninsular Ranges) exhibits concurrent flare ups during the Late Cretaceous (ca. 100–90 Ma) (Paterson and Ducea, 2015). Not all flare ups are correlated over such large distances (Kirsch et al., 2016), but these cases do raise the possibility that some flare ups may be related to large-scale geodynamic mechanisms. Below, we discuss a couple of mechanisms that have been proposed to influence slab dip at large-scales and allow periodic changes in slab dip, which could cause periodic arc migration.

Mantle tomography models indicate that subducted slabs tend to penetrate, stagnate, and fold in the mantle transition zone, particularly across the 660 km discontinuity where mantle viscosity increases and density increases due to phase transitions (Fukao and Obayashi, 2013; Goes et al., 2017). These observations have led to the development of geodynamic models that use slab behavior in the lower mantle to explain orogenic processes at strongly convergent plate margins, including changes in slab dip and plate coupling. There are two main, interrelated mechanisms that have been proposed to cause periodic slab-shallowing and could lead to an arc flare up. First, when a slab becomes anchored in the lower mantle, it may impede lateral migration and limit trench motion, causing increased convergence and the upper plate to “override” the trench, which results in a shallower slab dip in the upper mantle (Agrusta et al., 2017; Cerpa et al., 2018; Christensen, 1996; Guillaume et al., 2009; Heuret et al., 2007; Holt et al., 2015; Lallemand et al., 2008; Martinod et al., 2010; Schellart, 2008). This process may be enhanced by whole mantle flow following slab anchoring (Husson et al., 2012; Faccenna et al., 2013, 2017) and by the length of the anchored slab (Schellart, 2017). Slab break-off or fragmentation may free the anchored slab and restart the cycle (e.g., Haschke et al., 2002a, 2002b,

2006). The periodicity, if any, of slab anchoring and break-off is unknown, but the Nazca slab subducting beneath South America may be the best modern analog to gain insight into this process. The Nazca slab penetrated the lower mantle between 70 and 35 Ma (Faccenna et al., 2017; Chen et al., 2019) and presently shows no clear evidence for past break-off events (Portner et al., 2020; Rodríguez et al., 2021). If slab anchoring ultimately controls magmatic episodicity, it most likely operates on long time frames (> 50 Myr?), which could explain some long-period flare up intervals (Fig. 12D). For example, the average time between flare ups in the North and South American Cordillera during the Mesozoic is 60–80 Myr (Paterson and Ducea, 2015).

The second process that may explain periodic changes in slab dip near the plate interface is slab folding in the lower mantle (Billen and Arredondo, 2018; Cerpa et al., 2014; Garel et al., 2014; Gibert et al., 2012; Guillaume et al., 2009; Lee and King, 2011; Ribe et al., 2007; Stegman et al., 2010). Resistance to sinking across the 660 km discontinuity can cause a slab to fold back and forth, sometimes over itself, and produce oscillating episodes of slab shallowing and steepening. This process can act in concert with slab anchoring (e.g., Faccenna et al., 2017). Most numerical and analog modeling studies indicate that slab folding operates at periods of  $\leq 25$  Myr (Cerpa et al., 2014; Garel et al., 2014; Gibert et al., 2012; Guillaume et al., 2009; Lee and King, 2011) although Billen and Arredondo (2018) produced folding with periods as high as 50 Myr by increasing plate age (thickness) and mantle viscosity. Many convergent continental arcs exhibit flare ups separated by <50 Myr, which could be related to slab folding, changes in slab dip, and arc migration. For instance, the average time between flare ups in the Andes during the Cenozoic is 30–40 Myr (Haschke et al., 2002a, 2002b; Paterson and Ducea, 2015; Pepper et al., 2016). Fig. 12C schematically illustrates short-period cyclical arc migration related to slab folding.

## 12. A conceptual model for flare ups related to arc migration

We envision a scenario in which the interactions between long-period processes like slab anchoring, short-period processes like slab folding, and singular, “one-off,” events like subduction of a submarine ridge or oceanic plateau produce a unique history of slab dip changes and attendant migrations of the arc (Fig. 12). If landward arc migration is related to flare ups, then geologic records of arc flare ups may help to disentangle slab behavior and even deep mantle geodynamics. Below, we present a conceptual model for the tectonic evolution of strongly convergent Cordilleran orogenic systems that focuses on the potential role of arc migration driven by changes in slab dip (Fig. 13). The model has four stages, 1) lull, 2) advance, 3) flare up, and 4) retreat. The model shares many similarities with previous orogenic cyclicity models that seek to explain periodic geodynamic phenomenon (Collins and Richards, 2008; DeCelles et al., 2009; Faccenna et al., 2021; Folguera and Ramos, 2011; Horton, 2018; Ramos, 2009). Fig. 13 uses slab anchoring as an example of a long-period cyclical processes to illustrate what may drive periodic slab shallowing, however, the geologic phenomena predicted to occur in the upper plate (e.g., flare ups, shortening, extension, uplift) are the same regardless of the duration of slab shallowing and the mechanisms that may have caused that shallowing. The model shown in Fig. 13 is most applicable to continental arcs that exhibit long-period magmatic behavior like the Peninsular Ranges batholith that experienced flare ups at ~245 Ma, ~165 Ma, and ~ 85 Ma, a period of ca. 80 Myr (Paterson and Ducea, 2015).

The first stage in the conceptual model is the magmatic lull. Magmatic activity is concentrated on the trench side of the arc and the asthenospheric mantle wedge is the dominant mantle source. If the arc is built upon young, accreted terranes or oceanic basement (e.g., western Sierra Nevada batholith), then these arc rocks will have juvenile radiogenic isotopic compositions. Compared to flare up periods, arc magmas may have lower Sr/Y and La/Yb values that reflect relatively thin crust and less hydrous melt sources. Thin arc crust may cause the orogenic wedge to have a low taper (topographic slope + basal

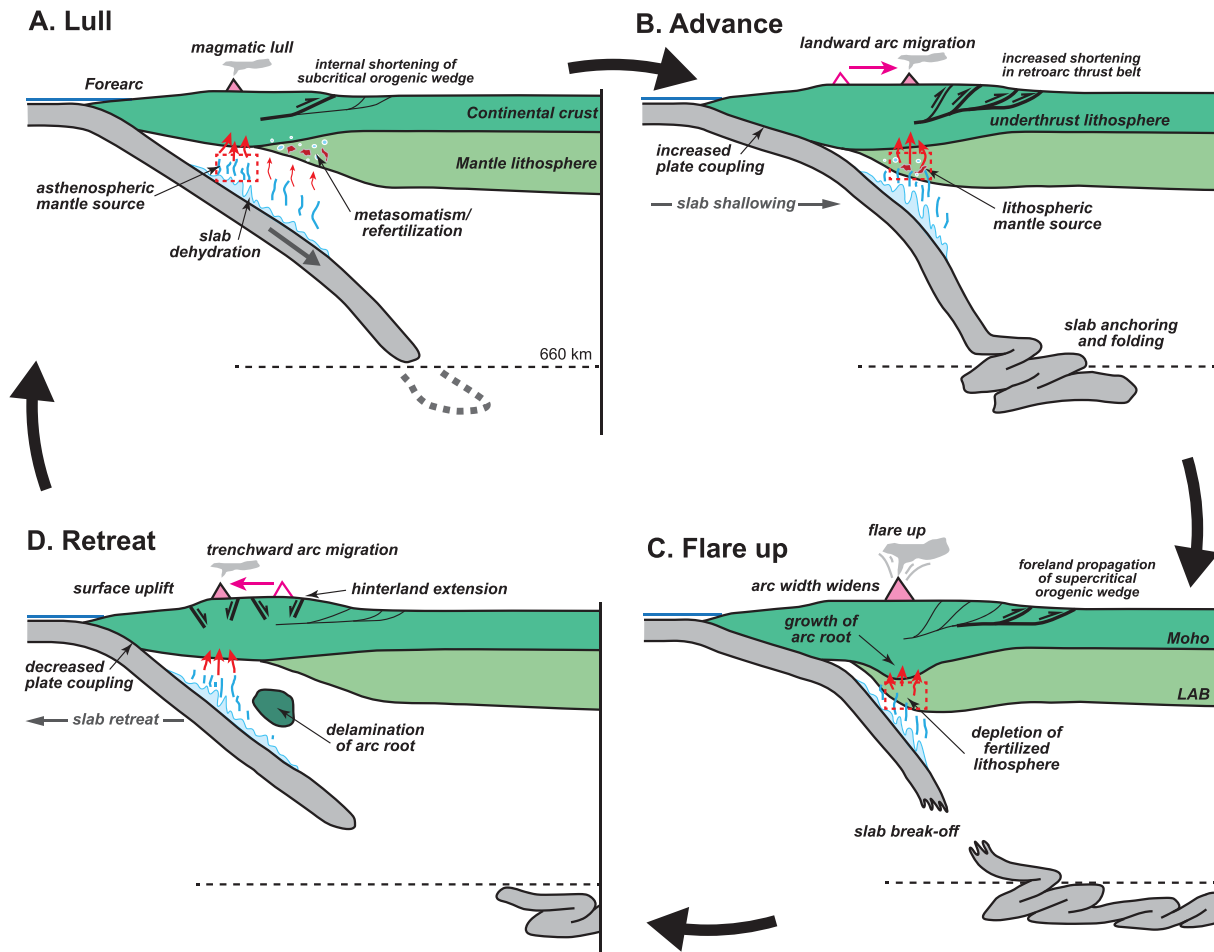


**Fig. 13.** A conceptual model illustrating how slab anchoring in the lower mantle can produce periodic slab shallowing, landward arc migration, arc flare ups, and explain deformation patterns in the upper plate. See text for details.

decollement dip angle) and to be in a subcritical state (Dahlen, 1990; Davis et al., 1983; DeCelles and Mitra, 1995; Platt, 1986). Out-of-sequence, contractional deformation is concentrated in the interior of the orogen (hinterland) to rebuild orogenic taper (e.g., DeCelles and Mitra, 1995). The subducting slab dips at a moderate angle. In terms of slab anchoring, this may represent a time when the slab has a free edge in the upper mantle (Fig. 13A). In terms of slab folding, this may represent a neutral interval between periods of landward slab folding and trenchward slab folding (Fig. 12). Fluids from the dehydrating slab and hydrous basaltic melts are 1) entrained into the magmatic plumbing system of the active arc and 2) emplaced into the mantle lithosphere in the back-arc region. The emplacement and storage of some mantle-derived melts in the mantle lithosphere suppresses arc crust production rates during the magmatic lull. The accumulation of metasomatic products in the mantle lithosphere also refertilizes the deep lithosphere.

Arc advance is the next stage in the conceptual model. Fig. 13B shows the slab penetrating and anchoring into the lower mantle, which causes increased plate coupling and slab shallowing in the upper mantle. Landward-directed slab folding in the lower mantle or subduction of more buoyant oceanic lithosphere (e.g., an oceanic plateau) may produce the same effects (Fig. 12). The shallowing of slab dip causes the arc to migrate landward and the source region for mantle-derived melts starts to include parts of the mantle lithosphere in addition to the mantle wedge. If the lithosphere is sufficiently old, the radiogenic isotopic composition of arc rocks becomes increasingly evolved during landward arc migration (Chapman et al., 2017). Otherwise, no significant change in isotopic composition is predicted. Increased plate coupling causes

contractional deformation to intensify throughout the orogenic wedge, including an increase in shortening in the retroarc thrust belt. Underthrusting of middle to lower crust beneath the retroarc and downward flow within the arc leads to crustal thickening (Cao et al., 2016; DeCelles et al., 2009; Paterson and Farris, 2008).

As the arc migrates farther landward, melting of refertilized mantle lithosphere becomes increasingly important and adds to melt production from the mantle wedge to produce an arc flare up event (Fig. 13C). The flare up activates more parts of the arc system and the width of the active arc increases (Fig. 11). Arc rocks may show a broader range of radiogenic isotopic compositions that are reflective of the wider arc and the age of the lithospheric provinces encountered. Repeated refertilization of the subcontinental mantle lithosphere and repeated flare ups in a single location in the arc system is predicted to produce subsequently more juvenile radiogenic isotope ratios. High rates of mantle-derived melt production lead to growth of a mafic to ultramafic arc root that complements felsic igneous rocks emplaced in the middle to upper crust (Ducea and Saleeby, 1998). Depletion of the mantle lithosphere and growth of this arc root contributes to extinguishing the flare up (Chin et al., 2015). Crustal thickening is achieved through a combination of magmatic and tectonic thickening (Cao et al., 2016), which leads to an increase in orogenic taper and a shift to a supercritical state. Active deformation and shortening is concentrated at the edge, or “toe,” of the orogenic wedge and new contractional faults propagate into the foreland, pushing the entire retroarc system (thrust belt + foreland basin) landward. Intra-arc shortening also reaches a maximum during the magmatic flare up stage (Cao et al., 2016; Paterson and Farris, 2008). If

slab anchoring is driving arc migration, the flare up stage may end when the connection between the subducting slab and anchored slab is broken (i.e., slab breakoff; Fig. 13C). If slab folding is driving arc migration, the stage may end when the slab begins to fold back toward the trench. If subduction of a buoyant feature drives arc migration, the flare up may end once the slab begins to re-steepen.

The final stage in the conceptual model is the retreat (steepening) of the slab in the upper mantle and the trenchward migration of the magmatic arc (Fig. 13D). Magma production rates drop and the value and range of radiogenic isotopic compositions of rocks returns to pre-flare up conditions. The depleted mantle wedge becomes increasingly important as the mantle source region. Slab retreat also reduces plate coupling and decreases horizontal stresses within the upper plate. The (over)thickened orogenic wedge may undergo extension and gravitational collapse (Wells and Hoisch, 2008) with extensional basins forming in the hinterland (Horton, 2018). Dense “arclogitic” arc roots may delaminate, leading to isostatic surface uplift that further increases gravitational potential energy and causes extension (Molnar et al., 1993). Extensional deformation is predicted despite the plate margin being in an overall convergent tectonic regime.

### 13. Conclusions

The causes of continental arc flare ups and magmatic lulls in convergent Cordilleran orogenic systems remains a first-order question in the Earth Sciences. Individual flare ups may be caused by a wide range of processes, but some arc flare ups share common characteristics, which suggests that there may be an underlying geodynamic or petrogenetic mechanism that drives changes in magma production. Continental arc flare ups often occur during landward arc migration and this migration pattern may start 10s of Myr before the flare up occurs. The migration of arcs into older, more evolved lithospheric provinces can produce a temporal shift toward more evolved radiogenic isotopic compositions in arc rocks. Without arc migration, the radiogenic isotopic composition at a single location within the arc system is predicted to show less variability. The width of the region of magmatic activity in an arc can expand significantly during a flare up and the range of radiogenic isotope ratios increases during flare ups as well. Contemporaneous magmatism across multiple lithospheric provinces or boundaries may help explain the wide range of isotope values. Continental arc magmatism is fundamentally related to melting of the mantle. The radiogenic isotopic composition of mantle xenoliths, exhumed mantle lithosphere, and of the least differentiated arc rocks located in the deep crust are particularly important for constraining the mantle source. Isotope studies indicate that primary, mantle-derived magmas generated during flare up events are often more evolved than the depleted mantle, which is interpreted to reflect substantial contributions from the mantle lithosphere.

Average arc crust production rates during arc flare ups are 70–90  $\text{km}^3 \text{km}^{-1} \text{Myr}^{-1}$  and  $< 20 \text{km}^3 \text{km}^{-1} \text{Myr}^{-1}$  during magmatic lulls. Arc crust production rates for individual intrusive suites emplaced during flare ups can be 100 s of  $\text{km}^3 \text{km}^{-1} \text{Myr}^{-1}$ . Part of this arc crust may be reworked from existing crust (generally ca. 50%), so long-term production rates for new, mantle-derived, continental crust is lower. However, mantle-derived melt production rates in continental arcs are appreciably higher than crust production rates because large volumes of mafic to ultramafic residual assemblages (i.e., arclogites) that were originally derived from the mantle are recycled, presumably by delamination. We estimate mantle-derived melt production rates for continental arcs to be 140–215  $\text{km}^3 \text{km}^{-1} \text{Myr}^{-1}$  during flare ups and  $\leq 15 \text{km}^3 \text{km}^{-1} \text{Myr}^{-1}$  during lulls. The difference in mantle-derived melt production between flare ups and lulls is large and difficult to explain simply by varying subduction parameters like plate convergence rate, slab dip, slab age, water flux from the slab, height of the mantle wedge, etc. Specifically, the difference is larger than the range of melt production rates predicted by models considering the full range of subduction

parameters observed globally. Compared to independent estimates for mantle melt production in subduction zones, these values suggest abnormally high mantle-derived melt production during flare ups and abnormally low melt production during lulls. When averaged out across a cycle alternating between flare ups and lulls, however, these rates are consistent with long-term independent estimates.

Previous studies have not focused on what may suppress magmatism during a lull. Intrusion and crystallization of mantle-derived melts that stall or pond in the lithospheric mantle is one mechanism that could reduce the amount of melt intruded into the deep crust. This process refertilizes the mantle lithosphere, which could become increasingly melt-fertile during magmatic lulls. Metasomatized mantle lithosphere may become more melt-fertile than primitive mantle and is capable of producing large volumes of basaltic magmas or even basaltic andesitic magmas. Partial melting of melt-fertile portions of the mantle lithosphere will significantly increase the amount of mantle-derived melt produced and may explain magma production rates during flare ups. Melt exhaustion, due to the large volumes of melt extracted from the mantle and growth of an arc root may also contribute to extinguishing a flare up.

If landward arc migration is related to flare ups, it is important to consider processes that cause migration. Slab shallowing is common during subduction of more buoyant oceanic lithosphere, but it may also be caused by interactions between subducted oceanic lithosphere and the mantle transition zone, including slab anchoring and slab folding. These processes can cause episodic changes in slab dip over timescales similar to flare ups and lulls in continental arcs. Changes in slab dip have been linked to a variety of geodynamic phenomena in Cordilleran orogenic systems such as alternating periods of contraction and extension. Investigations into the role of arc migration may help reconcile magmatic records of flare ups and lulls with these other geologic datasets.

The role of arc migration and the mantle lithosphere in producing continental arc flare ups was emphasized in this review, but there are many other topics that require further investigation. First, many tectonic processes correlate with slab-shallowing and arc migration, including sediment subduction and crustal thickening, which could generate flare ups. Holistic studies of interrelated geodynamic phenomenon in Cordilleran orogenic systems are needed to understand the interconnectedness of these processes. Second, flare ups occur in continental arcs that do not exhibit arc migration and these flare ups necessitate alternative models to explain high magmatic addition rates. There is no one-size-fits-all model to explain arc flare ups and examination of the unique characteristics of individual high-flux episodes are as equally likely to yield insight as studies of the commonalities. Third, many features of flare ups are yet to be rigorously scrutinized and/or compared across multiple arc systems, including flare up duration, changes in the volume of magmatism from one flare up to the next, and geochemical trends. Fourth, numerical models and experimental studies of mantle melting in subduction zones have not explored flare-up conditions and tend to focus exclusively on the asthenospheric mantle. Next, high magmatic addition rates and the episodic nature of flare ups and lulls may be unrelated to melt-production altogether and instead be caused by processes such as punctuated melt evacuation from deep crustal MASH zones and/or the mantle lithosphere. These systems may need to reach a critical melt fraction or connectivity threshold before large-scale melt extraction can occur. Finally, the differences and similarities between continental arc-type and ignimbrite-type flare ups in Cordilleran orogens should be explored. These flare ups are produced by different tectonic scenarios and processes, but the underlying petrologic mechanisms and conditions may be comparable.

### Declaration of Competing Interest

The authors declare that they have no known competing financial interests or personal relationships that could have appeared to influence

the work reported in this paper.

## Acknowledgements

J.B.C. acknowledges support from U.S. National Science Foundation (NSF) grant EAR 1946662. M.N.D. acknowledges support from U.S. NSF grants EAR 1725002 and EAR 2020935 and the Romanian Executive Agency for Higher Education, Research, Development, and Innovative Funding project PN-III-P4-ID-PCCF-2016-0014. S.R.P. acknowledges support from U.S. NSF grant EAR 1624847, EAR 1524798, and U.S.G.S EdMap grants G18AC00175 and G16AC00160. Constructive reviews by Joshua Schwartz, Shanaka de Silva, and editor Michael Roden greatly improved the manuscript.

## References

- Agrusta, R., Goes, S., van Hunen, J., 2017. Subducting-slab transition zone interaction: stagnation, penetration and mode switches. *Earth Planet. Sci. Lett.* 464, 10–23.
- Akinin, V.V., Miller, E.L., Toro, J., Prokopyev, A.V., Gottlieb, E.S., Pearce, S., Polzunenkov, G.O., Trunilina, V.A., 2020. Episodicity and the dance of late Mesozoic magmatism and deformation along the northern circum-pacific margin: Nerussia to the Cordillera. *Earth Sci. Rev.* 103272.
- Alasino, P.H., Casquet, C., Pankhurst, R.J., Rapela, C.W., Dahlquist, J.A., Galindo, C., Larrovere, M.A., Recio, C., Paterson, S.R., Colombo, F., Baldo, E.G., 2016. Mafic rocks of the Ordovician Famatinian magmatic arc (NW Argentina): New insights into the mantle contribution. *Geol. Soc. Am. Bull.* 128, 1105–1120.
- Alasino, P., Casquet, C., Galindo, C., Pankhurst, R., Rapela, C., Dahlquist, J., Recio, C., Baldo, E., Larrovere, M., Ramacciotti, C., 2020. O–H–Sr–Nd isotope constraints on the origin of the Famatinian magmatic arc, NW Argentina. *Geol. Mag.* 157, 2067–2080.
- Anders, E., Grevesse, N., 1989. Abundances of the elements: Meteoritic and solar. *Geochim. Cosmochim. Acta* 53, 197–214.
- Annen, C., Blundy, J.D., Leuthold, J., Sparks, R.S.J., 2015. Construction and evolution of igneous bodies: Towards an integrated perspective of crustal magmatism. *Lithos* 230, 206–221.
- Annen, C., Blundy, J.D., Sparks, R.S.J., 2006. The genesis of intermediate and silicic magmas in deep crustal hot zones. *J. Petrol.* 47, 505–539.
- Annen, C., Sparks, R.S.J., 2002. Effects of repetitive emplacement of basaltic intrusions on thermal evolution and melt generation in the crust. *Earth Planet. Sci. Lett.* 203, 937–955.
- Ardill, K.E., 2020. Spatial and Temporal Evolution of Magmatic Systems in Continental Arcs: A Case Study of Dynamic Arc Behaviors in the Mesozoic Sierra Nevada. University of Southern California, Ph.D. dissertation, California, p. 333.
- Ardill, K., Paterson, S., Memeti, V., 2018. Spatiotemporal magmatic focusing in upper-mid crustal plutons of the Sierra Nevada arc. *Earth Planet. Sci. Lett.* 498, 88–100.
- Armstrong, R.L., 1988. Mesozoic and early Cenozoic magmatic evolution of the Canadian Cordillera. *Geol. Soc. Am. Spec. Pap.* 218, 55–92.
- Attia, S., Cottle, J.M., Paterson, S.R., 2020. Erupted zircon record of continental crust formation during mantle driven arc flare-ups. *Geology* 48, 446–451.
- Baker, D.R., Alletti, M., 2012. Fluid saturation and volatile partitioning between melts and hydrous fluids in crustal magmatic systems: The contribution of experimental measurements and solubility models. *Earth Sci. Rev.* 114, 298–324.
- Barboza, S.A., Bergantz, G.W., 2000. Metamorphism and anatexis in the mafic complex contact aureole, Ivrea Zone, Northern Italy. *J. Petrol.* 41, 1307–1327.
- Bekaert, D.V., Turner, S.J., Broadley, M.W., Barnes, J.D., Halldórsson, S.A., Labidi, J., Wade, J., Walowski, K.J., Barry, P.H., 2020. Subduction-Driven Volatile Recycling: A Global Mass Balance. *Ann. Rev. Earth Planet. Sci.* 49.
- Beranek, L.P., McClelland, W.C., van Staal, C.R., Israel, S., Gordeev, S.M., 2017. Late Jurassic flare-up of the Coast Mountains arc system, NW Canada, and dynamic linkages across the northern Cordilleran orogen. *Tectonics* 36, 877–901.
- Best, M.G., Barr, D.L., Christiansen, E.H., Gromme, S., Deino, A.L., Tingey, D.G., 2009. The Great Basin Altiplano during the middle Cenozoic ignimbrite flareup: Insights from volcanic rocks. *Int. Geol. Rev.* 51, 589–633.
- Best, M.G., Christiansen, E.H., de Silva, S., Lipman, P.W., 2016. Slab-rollback ignimbrite flareups in the southern Great Basin and other Cenozoic American arcs: A distinct style of arc volcanism. *Geosphere* 12, 1097–1135.
- Billen, M.I., Arredondo, K.M., 2018. Decoupling of plate-asthenosphere motion caused by non-linear viscosity during slab folding in the transition zone. *Phys. Earth Planet. Inter.* 281, 17–30.
- Blatter, D.L., Carmichael, I.S., 1998. Hornblende peridotite xenoliths from Central Mexico reveal the highly oxidized nature of subarc upper mantle. *Geology* 26, 1035–1038.
- Bouilhol, P., Schaltegger, U., Chiaradia, M., Ovtcharova, M., Stracke, A., Burg, J.P., Dawood, H., 2011. Timing of juvenile arc crust formation and evolution in the Sapat complex (Kohistan–Pakistan). *Chem. Geol.* 280, 243–256.
- Brown, M., 2007. Crustal melting and melt extraction, ascent and emplacement in orogens: mechanisms and consequences. *J. Geol. Soc.* 164, 709–730.
- Brown, M., Averkin, Y.A., McLellan, E.L., Sawyer, E.W., 1995. Melt segregation in migmatites. *J. Geophys. Res.: Solid Earth* 100, 15655–15679.
- Bucholz, C.E., Jagoutz, O., VanTongeren, J.A., Setera, J., Wang, Z., 2017. Oxygen isotope trajectories of crystallizing melts: insights from modeling and the plutonic record. *Geochim. Cosmochim. Acta* 207, 154–184.
- Cagnioncle, A.-M., Parmentier, E.M., Elkins-Tanton, L.T., 2007. Effect of solid flow above a subducting slab on water distribution and melting at convergent plate boundaries. *J. Geophys. Res. Solid Earth* 112 (B9).
- Cao, W., Paterson, S., Memeti, V., Mundil, R., Anderson, J.L., Schmidt, K., 2015. Tracking paleodeformation fields in the Mesozoic central Sierra Nevada arc: Implications for intra-arc cyclic deformation and arc tempos. *Lithosphere* 7, 296–320.
- Cao, W., Paterson, S., Saleeby, J., Zalunardo, S., 2016. Bulk arc strain, crustal thickening, magma emplacement, and mass balances in the Mesozoic Sierra Nevada arc. *J. Struct. Geol.* 84, 14–30.
- Cao, W., Lee, C.T.A., Lackey, J.S., 2017. Episodic nature of continental arc activity since 750 Ma: A global compilation. *Earth Planet. Sci. Lett.* 461, 85–95.
- Cardona, A., León, S., Jaramillo, J.S., Montes, C., Valencia, V., Vanegas, J., Bustamante, C., Echeverri, S., 2018. The Paleogene arcs of the northern Andes of Colombia and Panama: insights on plate kinematic implications from new and existing geochemical, geochronological and isotopic data. *Tectonophysics* 749, 88–103.
- Carlson, R.L., Miller, D.J., 2003. Mantle wedge water contents estimated from seismic velocities in partially serpentinized peridotites. *Geophys. Res. Lett.* 30 (5).
- Castruccio, A., Rust, A.C., Sparks, R.S.J., 2010. Rheology and flow of crystal-bearing lavas: Insights from analogue gravity currents. *Earth Planet. Sci. Lett.* 297, 471–480.
- Cavazos-Tovar, J.G., Gómez-Tuena, A., Parolari, M., 2020. The origin and evolution of the Mexican Cordillera as registered in modern detrital zircons. *Gondwana Res.* 86, 83–103.
- Cawood, P.A., Kröner, A., Collins, W.J., Kusky, T.M., Mooney, W.D., Windley, B.F., 2009. Accretionary orogens through Earth history. *Geol. Soc. Lond. Spec. Publ.* 318, 1–36.
- Cecil, M.R., Rotberg, G.L., Ducea, M.N., Saleeby, J.B., Gehrels, G.E., 2012. Magmatic growth and batholithic root development in the northern Sierra Nevada, California. *Geosphere* 8, 592–606.
- Cecil, M.R., Rusmore, M.E., Gehrels, G.E., Woodsworth, G.J., Stowell, H.H., Yokelson, I. N., Chisom, C., Trautman, M., Homan, E., 2018. Along-strike variation in the magmatic tempo of the Coast Mountains Batholith, British Columbia, and implications for processes controlling episodicity in arcs. *Geochem. Geophys. Geosyst.* 19, 4274–4289.
- Cecil, M.R., Gehrels, G., Ducea, M.N., Patchett, P.J., 2011. U–Pb–Hf characterization of the central Coast Mountains batholith: Implications for petrogenesis and crustal architecture. *Lithosphere* 3, 247–260.
- Cecil, M.R., Gehrels, G.E., Yokelson, I.N., Homan, E., Rusmore, M.E., Stowell, H.H., Woodsworth, G.J., Valley, J.W., Kitajima, K., 2019, May. Zircon Hf and O isotope analysis of Jurassic-Eocene plutons of the southern Coast Mountains Batholith, British Columbia, indicates magmatic events dominated by mantle sources. In: Geological Society of America Annual Cordilleran Section Meeting, Abstracts with Programs, 51 n. 4.
- Cerpa, N.G., Hassani, R., Gerbault, M., Prévost, J.H., 2014. A fictitious domain method for lithosphere-asthenosphere interaction: Application to periodic slab folding in the upper mantle. *Geochem. Geophys. Geosyst.* 15, 1852–1877.
- Cerpa, N.G., Guillaume, B., Martinod, J., 2018. The interplay between overriding plate kinematics, slab dip and tectonics. *Geophys. J. Int.* 215, 1789–1802.
- Cerpa, N.G., Wada, I., Wilson, C.R., 2019. Effects of fluid influx, fluid viscosity, and fluid density on fluid migration in the mantle wedge and their implications for hydrous melting. *Geosphere* 15, 1–23.
- Chaharlang, R., Ducea, M.N., Ghalamghash, J., 2020. Geochemical evidences for quantifying crustal thickness over time in the Urumieh-Dokhtar magmatic arc (Iran). *Lithos* 374 (105723).
- Chapman, J.B., Ducea, M.N., 2019. The role of arc migration in Cordilleran orogenic cyclicity. *Geology* 47, 627–631.
- Chapman, J.B., Kapp, P., 2017. Tibetan magmatism database. *Geochem. Geophys. Geosyst.* 18, 4229–4234.
- Chapman, A.D., Saleeby, J.B., Eiler, J., 2013. Slab flattening trigger for isotopic disturbance and magmatic flare-up in the southernmost Sierra Nevada batholith, California. *Geology* 41, 1007–1010.
- Chapman, A.D., Ducea, M.N., Kidder, S., Petrescu, L., 2014. Geochemical constraints on the petrogenesis of the Salinian arc, Central California: Implications for the origin of intermediate magmas. *Lithos* 200, 126–141.
- Chapman, J.B., Ducea, M.N., DeCelles, P.G., Profeta, L., 2015. Tracking changes in crustal thickness during orogenic evolution with Sr/Y: An example from the North American Cordillera. *Geology* 43, 919–922.
- Chapman, J.B., Ducea, M.N., Kapp, P., Gehrels, G.E., DeCelles, P.G., 2017. Spatial and temporal radiogenic isotopic trends of magmatism in Cordilleran orogens. *Gondwana Res.* 48, 189–204.
- Chapman, J.B., Scoggin, S.H., Kapp, P., Carrapa, B., Ducea, M.N., Worthington, J., Oimahmadov, I., Gadoev, M., 2018. Mesozoic to Cenozoic magmatic history of the Pamir. *Earth Planet. Sci. Lett.* 482, 181–192.
- Chen, J.H., Moore, J.G., 1982. Uranium-lead isotopic ages from the Sierra Nevada Batholith, California. *J. Geophys. Res. Solid Earth* 87, 4761–4784.
- Chen, Y.W., Wu, J., Suppe, J., 2019. Southward propagation of Nazca subduction along the Andes. *Nature* 565, 441–447.
- Chin, E.J., Lee, C.T.A., Luffi, P., Tice, M., 2012. Deep lithospheric thickening and fertilization beneath continental arcs: Case study of the P, T and compositional evolution of peridotite xenoliths from the Sierra Nevada, California. *J. Petrol.* 53, 477–511.
- Cheong, A.C.S., Jo, H.J., 2020. Tectonomagmatic evolution of a Jurassic Cordilleran flare-up along the Korean Peninsula: Geochronological and geochemical constraints from granitoid rocks. *Gondwana Research* 88, 21–44.

- Chin, E.J., Lee, C.T.A., Barnes, J.D., 2014. Thickening, refertilization, and the deep lithosphere filter in continental arcs: Constraints from major and trace elements and oxygen isotopes. *Earth Planet. Sci. Lett.* 397, 184–200.
- Chin, E.J., Lee, C.T.A., Blichert-Toft, J., 2015. Growth of upper plate lithosphere controls tempo of arc magmatism: Constraints from Al-diffusion kinetics and coupled Lu-Hf and Sm-Nd chronology. *Geochem. Perspect. Lett.* 1, 20–32.
- Christensen, U.R., 1996. The influence of trench migration on slab penetration into the lower mantle. *Earth Planet. Sci. Lett.* 140, 27–39.
- Clemens, J.D., Stevens, G., 2016. Melt segregation and magma interactions during crustal melting: breaking out of the matrix. *Earth Sci. Rev.* 160, 333–349.
- Clift, P.D., Vannucchi, P., 2004. Controls on tectonic accretion versus erosion in subduction zones: implications for the origin and recycling of the continental crust. *Rev. Geophys.* 42 (2).
- Coira, B., Davidson, J., Mpodozis, C., Ramos, V., 1982. Tectonic and magmatic evolution of the Andes of northern Argentina and Chile. *Earth Sci. Rev.* 18, 303–332.
- Collins, W.J., 2002. Hot orogens, tectonic switching, and creation of continental crust. *Geology* 30, 535–538.
- Collins, W.J., Richards, S.W., 2008. Geodynamic significance of S-type granites in circum-Pacific orogens. *Geology* 36, 559–562.
- Coney, P.J., Reynolds, S.J., 1977. Cordilleran benioff zones. *Nature* 270, 403–406.
- Connolly, J.A.D., Podladchikov, Y.Y., 2007. Decompression weakening and channeling instability in ductile porous media: Implications for asthenospheric melt segregation. *J. Geophys. Res.: Solid Earth* 112.
- Connolly, J.A., Schmidt, M.W., Solferino, G., Bagdassarov, N., 2009. Permeability of asthenospheric mantle and melt extraction rates at mid-ocean ridges. *Nature* 462, 209–212.
- Cope, T., 2017. Phanerozoic magmatic tempos of North China. *Earth Planet. Sci. Lett.* 468, 1–10.
- Costa, A., Caricchi, L., Bagdassarov, N., 2009. A model for the rheology of particle-bearing suspensions and partially molten rocks. *Geochem. Geophys. Geosyst.* 10.
- Crisp, J.A., 1984. Rates of magma emplacement and volcanic output. *J. Volcanol. Geotherm. Res.* 20, 177–211.
- Czertowicz, T.A., Scott, J.M., Waight, T.E., Palin, J.M., Van der Meer, Q.H.A., Le Roux, P., Münker, C., Piazzolo, S., 2016. The Anita Peridotite, New Zealand: ultra-depletion and subtle enrichment in sub-arc mantle. *J. Petrol.* 57, 717–750.
- Dafu, M.N., Carrera, A., Gehrels, G.E., Alberts, D., Pereira, M., Cecil, M.R., Rusmore, M.E., Stowell, H.H., Woodsworth, G.J., Roeske, S.M., 2020. U-Th-Pb geochronology and Lu-Hf isotope geochemistry of detrital zircons in metasedimentary rocks of the Southern Coast Mountains Batholith. *Lithosphere* 1 (8854686).
- Dahlen, F.A., 1990. Critical taper model of fold-and-thrust belts and accretionary wedges. *Annu. Rev. Earth Planet. Sci.* 18, 55–99.
- Davidson, J., Turner, S., Handley, H., Macpherson, C., Dosseto, A., 2007. Amphibole “sponge” in arc crust? *Geology* 35, 787–790.
- Davies, J.H., Stevenson, D.J., 1992. Physical model of source region of subduction zone volcanics. *J. Geophys. Res. Solid Earth* 97, 2037–2070.
- Davis, J., Hawkesworth, C., 1993. The petrogenesis of 30–20 Ma basic and intermediate volcanics from the Mogollon-Datil volcanic field, New-Mexico, USA. *Contrib. Mineral. Petrol.* 115, 165–183.
- Davis, D., Suppe, J., Dahlen, F.A., 1983. Mechanics of fold-and-thrust belts and accretionary wedges. *J. Geophys. Res. Solid Earth* 88, 1153–1172.
- de Bremond d’Ars, J., Jaupart, C., Sparks, R.S.J., 1995. Distribution of volcanoes in active margins. *J. Geophys. Res.* 100, 20421–20432.
- de Silva, S.L., Kay, S.M., 2018. Turning up the heat: high-flux magmatism in the Central Andes. *Elements* 14, 245–250.
- de Silva, S.L., Riggs, N.R., Barth, A.P., 2015. Quickening the pulse: fractal tempos in continental arc magmatism. *Elements* 11, 113–118.
- DeCelles, P.G., Graham, S.A., 2015. Cyclical processes in the north American Cordilleran orogenic system. *Geology* 43, 499–502.
- DeCelles, P.G., Mitra, G., 1995. History of the Sevier orogenic wedge in terms of critical taper models, Northeast Utah and Southwest Wyoming. *Geol. Soc. Am. Bull.* 107, 454–462.
- DeCelles, P.G., Ducea, M.N., Kapp, P., Zandt, G., 2009. Cyclicity in Cordilleran orogenic systems. *Nat. Geosci.* 2, 251–257.
- DeCelles, P.G., Zandt, G., Beck, S.L., Currie, C.A., Ducea, M.N., Kapp, P., Gehrels, G.E., Carrapa, B., Quade, J., Schoenbohm, L.M., 2015. Cyclical orogenic processes in the Cenozoic Central Andes. In: DeCelles, P.G., Ducea, M.N., Carrapa, B., Kapp, P.A. (Eds.), *Geodynamics of a Cordilleran Orogenic System: The Central Andes of Argentina and Northern Chile*, 212. Geological Society of America Memoir, pp. 459–490.
- Decker, M., Schwartz, J., Stowell, H., Klepeis, K., Tulloch, A., Kitajima, K., Valley, J., Kylander-Clark, A., 2017. Slab-triggered arc flare-up in the Cretaceous median Batholith and the growth of lower arc crust, Fiordland, New Zealand. *J. Petrol.* 58, 1145–1171.
- del Rey, A., Deckart, K., Arriagada, C., Martínez, F., 2016. Resolving the paradigm of the late Paleozoic–Triassic Chilean magmatism: Isotopic approach. *Gondwana Res.* 37, 172–181.
- DePaolo, D.J., Harrison, T.M., Wielicki, M., Zhao, Z., Zhu, D.C., Zhang, H., Mo, X., 2019. Geochemical evidence for thin syn-collision crust and major crustal thickening between 45 and 32 Ma at the southern margin of Tibet. *Gondwana Res.* 73, 123–135.
- Dickinson, W.R., Snyder, W.S., Matthews, V., 1978. Plate tectonics of the Laramide orogeny. In: Matthews, V. (Ed.), *Laramide Folding Associated with Basement Block Faulting in the Western United States*, 151. Geological Society of America Memoir, pp. 355–366.
- Dimalanta, C., Taira, A., Yumul Jr., G.P., Tokuyama, H., Mochizuki, K., 2002. New rates of western Pacific island arc magmatism from seismic and gravity data. *Earth Planet. Sci. Lett.* 202, 105–115.
- Ducea, M.N., 2001. The California arc: Thick granitic batholiths, eclogitic residues, lithospheric-scale thrusting, and magmatic flare-ups. *GSA Today* 11, 4–10.
- Ducea, M.N., 2002. Constraints on the bulk composition and root foundering rates of continental arcs: A California arc perspective. *J. Geophys. Res.: Solid Earth* 107, 2304.
- Ducea, M.N., Barton, M.D., 2007. Igniting flare-up events in Cordilleran arcs. *Geology* 35, 1047–1050.
- Ducea, M.N., Bergantz, G.W., Crowley, J.L., Otamendi, J., 2017. Ultrafast magmatic buildup and diversification to produce continental crust during subduction. *Geology* 45, 235–238.
- Ducea, M.N., Chapman, A.D., 2018. Sub-magmatic arc underplating by trench and forearc materials in shallow subduction systems; a geologic perspective and implications. *Earth Sci. Rev.* 185, 763–779.
- Ducea, M.N., Saleeby, J.B., 1996. Buoyancy sources for a large, unrooted mountain range, the Sierra Nevada, California: evidence from xenolith thermobarometry. *J. Geophys. Res. Solid Earth* 101, 8229–8244.
- Ducea, M.N., Saleeby, J.B., 1998. The age and origin of a thick mafic-ultramafic keel from beneath the Sierra Nevada batholith. *Contrib. Mineral. Petrol.* 133, 169–185.
- Ducea, M.N., Chapman, A.D., Bowman, E., Tryantafyllou, A., 2020a. Arclogites and their role in continental evolution; part 1: Background, locations, petrography, geochemistry, chronology and thermobarometry. *Earth Sci. Rev.*, 103375.
- Ducea, M.N., Chapman, A.D., Bowman, E., Balica, C., 2020b. Arclogites and their role in continental evolution; part 2: relationship to batholiths and volcanoes, density and foundering, remelting and long-term storage in the mantle. *Earth Sci. Rev.* 214 (103476) n. 103476.
- Ducea, M.N., Kidder, S., Chesley, J.T., Saleeby, J.B., 2009. Tectonic underplating of trench sediments beneath magmatic arcs: the central California example. *Int. Geol. Rev.* 51, 1–26.
- Ducea, M.N., Paterson, S.R., DeCelles, P.G., 2015a. High-volume magmatic events in subduction systems. *Elements* 11, 99–104.
- Ducea, M.N., Saleeby, J.B., Bergantz, G., 2015b. The architecture, chemistry, and evolution of continental magmatic arcs. *Annu. Rev. Earth Planet. Sci.* 43 (10–11).
- Dufek, J., Bergantz, G.W., 2005. Lower crustal magma genesis and preservation: a stochastic framework for the evaluation of basalt–crust interaction. *J. Petrol.* 46, 2167–2195.
- Echaurren, A., Gianni, G.M., Paz, L.F., Navarrete, C., Oliveros, V., Encinas, A., Giménez, M., Lince-Klinger, F., Folguera, A., 2019. Tectonic controls on the building of the North Patagonian fold-thrust belt (~ 43° S). In: Horton, B., Folguera, A. (Eds.), *Andean Tectonics*. Elsevier, pp. 609–650.
- Eiler, J.M., 2001. Oxygen isotope variations of basaltic lavas and upper mantle rocks. *Rev. Mineral. Geochem.* 43, 319–364.
- England, P.C., Katz, R.F., 2010. Melting above the anhydrous solidus controls the location of volcanic arcs. *Nature* 467, 700–703.
- Ersoy, E.Y., Helvacı, C., Palmer, M.R., 2010. Mantle source characteristics and melting models for the early-middle Miocene mafic volcanism in Western Anatolia: implications for enrichment processes of mantle lithosphere and origin of K-rich volcanism in post-collisional settings. *J. Volcanol. Geotherm. Res.* 198, 112–128.
- Faccenna, C., Becker, T.W., Conrad, C.P., Husson, L., 2013. Mountain building and mantle dynamics. *Tectonics* 32, 80–93.
- Faccenna, C., Becker, T.W., Holt, A.F., Brun, J.P., 2021. Mountain building, mantle convection, and supercontinents: revisited. *Earth Planet. Sci. Lett.* 564 (116905).
- Faccenna, C., Oncken, O., Holt, A.F., Becker, T.W., 2017. Initiation of the Andean orogeny by lower mantle subduction. *Earth Planet. Sci. Lett.* 463, 189–201.
- Farmer, G.L., Bailey, T., Elkins-Tanton, L.T., 2008. Mantle source volumes and the origin of the mid-Tertiary ignimbrite flare-up in the southern Rocky Mountains, western US. *Lithos* 102, 279–294.
- Farner, M.J., Lee, C.T.A., 2017. Effects of crustal thickness on magmatic differentiation in subduction zone volcanism: a global study. *Earth Planet. Sci. Lett.* 470, 96–107.
- Ferrari, L., López-Martínez, M., Rosas-Elguera, J., 2002. Ignimbrite flare-up and deformation in the southern Sierra Madre Occidental, western Mexico: implications for the late subduction history of the Farallon plate. *Tectonics* 21 (17).
- Folguera, A., Ramos, V.A., 2011. Repeated eastward shifts of arc magmatism in the Southern Andes: a revision to the long-term pattern of Andean uplift and magmatism. *J. S. Am. Earth Sci.* 32, 531–546.
- Freyer, H., Brandmeier, M., Wörner, G., 2015. The origin and crust/mantle mass balance of Central Andean ignimbrite magmatism constrained by oxygen and strontium isotopes and erupted volumes. *Contrib. Mineral. Petrol.* 169, 1–24.
- Fukao, Y., Obayashi, M., 2013. Subducted slabs stagnant above, penetrating through, and trapped below the 660 km discontinuity. *J. Geophys. Res. Solid Earth* 118, 5920–5938.
- Ganade, C.E., Cordani, U.G., Weinberg, R.F., Basei, M.A., Armstrong, R., Sato, K., 2014. Tracing Neoproterozoic subduction in the Borborema Province (NE-Brazil): Clues from U-Pb geochronology and Sr-Nd-Hf-O isotopes on granitoids and migmatites. *Lithos* 202, 167–189.
- Ganade, C.E., Lanari, P., Rubatto, D., Hermann, J., Weinberg, R.F., Basei, M.A.S., Tesser, L.R., Caby, R., Agbossoumonde, Y., Ribeiro, C.M., 2021. Magmatic flare-up causes crustal thickening at the transition from subduction to continental collision. *Commun. Earth Environ.* 2 (41).
- Garel, F., Goes, S., Davies, D.R., Davies, J.H., Kramer, S.C., Wilson, C.R., 2014. Interaction of subducted slabs with the mantle transition-zone: a regime diagram from 2-D thermo-mechanical models with a mobile trench and an overriding plate. *Geochem. Geophys. Geosyst.* 15, 1739–1765.
- Gehrels, G., Rusmore, M., Woodsworth, G., Crawford, M., Andronico, C., Hollister, L., Patchett, J., Ducea, M., Butler, R., Klepeis, K., Davidson, C., 2009. U-Th-Pb geochronology of the Coast Mountains batholith in north-coastal British Columbia: Constraints on age and tectonic evolution. *Geol. Soc. Am. Bull.* 121, 1341–1361.

- Gerya, T.V., Meilick, F.I., 2011. Geodynamic regimes of subduction under an active margin: effects of rheological weakening by fluids and melts. *J. Metamorph. Geol.* 29, 7–31.
- Gerya, T.V., Yuen, D.A., 2003. Rayleigh–Taylor instabilities from hydration and melting propel ‘cold plumes’ at subduction zones. *Earth Planet. Sci. Lett.* 212, 47–62.
- Ghiorso, M.S., Hirschmann, M.M., Reiners, P.W., Kress, V.C., 2002. The pMELTS: a revision of MELTS for improved calculation of phase relations and major element partitioning related to partial melting of the mantle to 3 GPa. *Geochemistry, Geophysics, Geosystems*, v. 3, 1–35.
- Gianni, G.M., Luján, S.P., 2021. Geodynamic controls on magmatic arc migration and quiescence. *Earth Sci. Rev.* 103676.
- Gianni, G.M., Dávila, F.M., Echaurren, A., Fennell, L., Tobal, J., Navarrete, C., Quezada, P., Folguera, A., Giménez, M., 2018. A geodynamic model linking Cretaceous orogeny, arc migration, foreland dynamic subsidence and marine incursion in southern South America. *Earth Sci. Rev.* 185, 437–462.
- Gibert, G., Gerbault, M., Hassani, R., Tric, E., 2012. Dependency of slab geometry on absolute velocities and conditions for cyclicity: insights from numerical modelling. *Geophys. J. Int.* 189, 747–760.
- Girardi, J.D., Patchett, P.J., Ducea, M.N., Gehrels, G.E., Cecil, M.R., Rusmore, M.E., Woodsworth, G.J., Pearson, D.M., Manthei, C., Wetmore, P., 2012. Elemental and isotopic evidence for granitoid genesis from deep-seated sources in the Coast Mountains Batholith, British Columbia. *J. Petrol.* 53, 1505–1536.
- Glen, R.A., 2013. Refining accretionary orogen models for the Tasmanides of eastern Australia. *Aust. J. Earth Sci.* 60, 315–370.
- Goes, S., Agrusta, R., van Hunen, J., Garel, F., 2017. Subduction-transition zone interaction: A review. *Geosphere* 13, 644–664.
- Grove, T.L., Chatterjee, N., Parman, S.W., Médard, E., 2006. The influence of H<sub>2</sub>O on mantle wedge melting. *Earth Planet. Sci. Lett.* 249, 74–89.
- Grove, T.L., Till, C.B., 2019. H 2 O-rich mantle melting near the slab–wedge interface. *Contrib. Mineral. Petrol.* 174, 1–22.
- Grove, T.L., Till, C.B., Krawczynski, M.J., 2012. The role of H<sub>2</sub>O in subduction zone magmatism. *Annu. Rev. Earth Planet. Sci.* 40, 413–439.
- Grunder, A.L., 1995. Material and thermal roles of basalt in crustal magmatism: Case study from eastern Nevada. *Geology* 23, 952–956.
- Guillaume, B., Martinod, J., Espurt, N., 2009. Variations of slab dip and overriding plate tectonics during subduction: Insights from analogue modelling. *Tectonophysics* 463, 167–174.
- Halama, R., Savov, I.P., Rudnick, R.L., McDonough, W.F., 2009. Insights into Li and Li isotope cycling and sub-arc metasomatism from veined mantle xenoliths, Kamchatka. *Contrib. Mineral. Petrol.* 158, 197–222.
- Harry, D.L., Leeman, W.P., 1995. Partial melting of melt metasomatized subcontinental mantle and the magma source potential of the lower lithosphere. *J. Geophys. Res. Solid Earth* 100, 10255–10269.
- Haschke, M., Siebel, W., Günther, A., Scheuber, E., 2002a. Repeated crustal thickening and recycling during the Andean orogeny in north Chile (21–26 S). *J. Geophys. Res. Solid Earth* 107 (ECV-6).
- Haschke, M.R., Scheuber, E., Günther, A., Reutter, K.J., 2002b. Evolutionary cycles during the Andean orogeny: repeated slab breakoff and flat subduction? *Terra Nova* 14, 49–55.
- Haschke, M., Günther, A., Melnick, D., Ehtler, H., Reutter, K.J., Scheuber, E., Oncken, O., 2006. Central and southern Andean tectonic evolution inferred from arc magmatism. In: Oncken, O., Chong, G., Franz, G., Giese, P., Götze, H.J., Ramos, V.A., Strecker, M.R., Wigger, P. (Eds.), *The Andes*. Springer, Berlin, Heidelberg, pp. 337–353.
- Hawkesworth, C., Cawood, P.A., Dhuime, B., 2019. Rates of generation and growth of the continental crust. *Geosci. Front.* 10, 165–173.
- Hebert, L.B., Antoshechkina, P., Asimow, P., Gurnis, M., 2009. Emergence of a low-viscosity channel in subduction zones through the coupling of mantle flow and thermodynamics. *Earth Planet. Sci. Lett.* 278, 243–256.
- Hervé, F., Fanning, C.M., Calderón, M., Mpodozis, C., 2014. Early Permian to late Triassic batholiths of the Chilean Frontal Cordillera (28°–31°S): SHRIMP U–Pb zircon ages and Lu–Hf and O isotope systematics. *Lithos* 184, 436–446.
- Heuret, A., Funicello, F., Faccenna, C., Lallemand, S., 2007. Plate kinematics, slab shape and back-arc stress: a comparison between laboratory models and current subduction zones. *Earth Planet. Sci. Lett.* 256, 473–483.
- Hildreth, W., Moorbath, S., 1988. Crustal contributions to arc magmatism in the Andes of central Chile. *Contrib. Mineral. Petrol.* 98, 455–489.
- Holt, A.F., Becker, T.W., Buffett, B.A., 2015. Trench migration and overriding plate stress in dynamic subduction models. *Geophys. J. Int.* 201, 172–192.
- Horton, B.K., 2018. Tectonic regimes of the central and southern Andes: responses to variations in plate coupling during subduction. *Tectonics* 37, 402–429.
- Horton, B.K., Fuentes, F., 2016. Sedimentary record of plate coupling and decoupling during growth of the Andes. *Geology* 44, 647–650.
- Hughes, G.R., Mahood, G.A., 2008. Tectonic controls on the nature of large silicic calderas in volcanic arcs. *Geology* 36, 627–630.
- Humphreys, E., Hessler, E., Dueker, K., Farmer, G.L., Erslev, E., Atwater, T., 2003. How Laramide-age hydration of north American lithosphere by the Farallon slab controlled subsequent activity in the western United States. *Int. Geol. Rev.* 45, 575–595.
- Huntington, K.W., Klepeis, K.A., with 66 community contributors, 2018. Challenges and opportunities for research in tectonics: Understanding deformation and the processes that link Earth systems, from geologic time to human time. In: *A Community Vision Document Submitted to the U.S. National Science Foundation: University of Washington*, p. 84.
- Husson, L., Conrad, C.P., Faccenna, C., 2012. Plate motions, Andean orogeny, and volcanism above the South Atlantic convection cell. *Earth Planet. Sci. Lett.* 317, 126–135.
- Ingebritsen, S.E., Sherrod, D.R., Mariner, R.H., 1989. Heat flow and hydrothermal circulation in the Cascade Range, north-Central Oregon. *Science* 243, 1458–1462.
- Jackson, M.D., Blundy, J., Sparks, R.S.J., 2018. Chemical differentiation, cold storage and remobilization of magma in the Earth’s crust. *Nature* 564, 405–409.
- Jagoutz, O., 2014. Arc crustal differentiation mechanisms. *Earth Planet. Sci. Lett.* 396, 267–277.
- Jagoutz, O., Kelemen, P.B., 2015. Role of arc processes in the formation of continental crust. *Annu. Rev. Earth Planet. Sci.* 43, 363–404.
- Jagoutz, O., Müntener, O., Burg, J.P., Ulmer, P., Jagoutz, E., 2006. Lower continental crust formation through focused flow in km-scale melt conduits: the zoned ultramafic bodies of the Chilas complex in the Kohistan island arc (NW Pakistan). *Earth Planet. Sci. Lett.* 242, 320–342.
- Jagoutz, O., Schmidt, M.W., 2013. The composition of the foundered complement to the continental crust and a re-evaluation of fluxes in arcs. *Earth Planet. Sci. Lett.* 371, 177–190.
- Ji, W.Q., Wu, F.Y., Chung, S.L., Li, J.X., Liu, C.Z., 2009. Zircon U–Pb geochronology and Hf isotopic constraints on petrogenesis of the Gangdese batholith, southern Tibet. *Chem. Geol.* 262, 229–245.
- Jiang, H., Lee, C.T.A., 2017. Coupled magmatism–erosion in continental arcs: reconstructing the history of the Cretaceous Peninsular Ranges batholith, southern California through detrital hornblende barometry in forearc sediments. *Earth Planet. Sci. Lett.* 472, 69–81.
- Jicha, B., Jagoutz, O., 2015. Magma production rates for intraoceanic arcs. *Elements* 11, 105–111.
- Jicha, B.R., Kay, S.M., 2018. Quantifying arc migration and the role of forearc subduction erosion in the central Aleutians. *J. Volcanol. Geotherm. Res.* 360, 84–99.
- Jicha, B.R., Scholl, D.W., Singer, B.S., Yagodinski, G.M., Kay, S.M., 2006. Revised age of Aleutian Island Arc formation implies high rate of magma production. *Geology* 34, 661–664.
- Jordan, T.E., Isacks, B.L., Allmendinger, R.W., Brewer, J.A., Ramos, V.A., Ando, C.J., 1983. Andean tectonics related to geometry of subducted Nazca plate. *Geol. Soc. Am. Bull.* 94, 341–361.
- Kapp, P., DeCelles, P.G., 2019. Mesozoic–Cenozoic geological evolution of the Himalayan–Tibetan orogen and working tectonic hypotheses. *Am. J. Sci.* 319, 159–254.
- Karlstrom, L., Lee, C.T., Manga, M., 2014. The role of magmatically driven lithospheric thickening on arc front migration. *Geochem. Geophys. Geosys.* 15, 2655–2675.
- Katz, R.F., Spiegelman, M., Langmuir, C.H., 2003. A new parameterization of hydrous mantle melting. *Geochem. Geophys. Geosyst.* 4 (9).
- Kay, S.M., Godoy, E., Kurtz, A., 2005. Episodic arc migration, crustal thickening, subduction erosion, and magmatism in the south-Central Andes. *Geol. Soc. Am. Bull.* 117, 67–88.
- Kay, S.M., Coira, B.L., Caffè, P.J., Chen, C.H., 2010. Regional chemical diversity, crustal and mantle sources and evolution of central Andean Puna plateau ignimbrites. *J. Volcanol. Geotherm. Res.* 198, 81–111.
- Kelley, K.A., Plank, T., Newman, S., Stolper, E.M., Grove, T.L., Parman, S., Hauri, E.H., 2010. Mantle melting as a function of water content beneath the Mariana Arc. *J. Petrol.* 51, 1711–1738.
- Kemp, A.I.S., Hawkesworth, C.J., Collins, W.J., Gray, C.M., Blevin, P.L., 2009. Isotopic evidence for rapid continental growth in an extensional accretionary orogen: The Tasmanides, eastern Australia. *Earth Planet. Sci. Lett.* 284, 455–466.
- Keppie, D.F., Currie, C.A., Warren, C., 2009. Subduction erosion modes: comparing finite element numerical models with the geological record. *Earth Planet. Sci. Lett.* 287, 241–254.
- Kidder, S., Ducea, M., Gehrels, G., Patchett, P.J., Vervoort, J., 2003. Tectonic and magmatic development of the Salinian Coast Ridge belt, California. *Tectonics* 22 (5).
- Kim, S.W., Kwon, S., Park, S.I., Lee, C., Cho, D.L., Lee, H.J., Ko, K., Kim, S.J., 2016. SHRIMP U–Pb dating and geochemistry of the Cretaceous plutonic rocks in the Korean Peninsula: a new tectonic model of the Cretaceous Korean Peninsula. *Lithos* 262, 88–106.
- Kim, S.W., Kwon, S., Jeong, Y.J., Kee, W.S., Lee, B.C., Byun, U.H., Ko, K., Cho, D.L., Hong, P.S., Park, S.I., Santosh, M., 2020. The middle Permian to Triassic tectono-magmatic system in the southern Korean Peninsula. *Gondwana Res.* 262, 88–106.
- King, R.L., Bebout, G.E., Moriguti, T., Nakamura, E., 2006. Elemental mixing systematics and Sr–Nd isotope geochemistry of mélange formation: obstacles to identification of fluid sources to arc volcanics. *Earth Planet. Sci. Lett.* 246, 288–304.
- Kirsch, M., Paterson, S.R., Wobbe, F., Ardila, A.M.M., Clausen, B.L., Alasino, P.H., 2016. Temporal histories of Cordilleran continental arcs: testing models for magmatic episodicity. *Am. Mineral.* 101, 2133–2154.
- Kistler, R.W., 1990. Two different lithosphere types in the Sierra Nevada, California. In: Anderson, J.L. (Ed.), *The Nature and Origin of Cordilleran Magmatism*, 174. Geological Society of America Memoir, pp. 271–281.
- Kistler, R.W., Wooden, J.L., Morton, D.M., 2003. Isotopes and ages in the northern Peninsular Ranges batholith, southern California: U.S. Geological Survey. In: *Open-File Report 03-489*, p. 45.
- Kistler, R.W., Wooden, J.L., Premo, W.R., Morton, D.M., Miller, F.K., 2014. Pb–Sr–Nd–O isotopic characterization of Mesozoic rocks throughout the northern end of the Peninsular Ranges batholith: Isotopic evidence for the magmatic evolution of oceanic arc–continental margin accretion during the Late Cretaceous of southern California. *Peninsular Ranges Batholith, Baja California and Southern California*. In: Morton, D.M., Miller, F.K. (Eds.), *Peninsular Ranges Batholith, Baja California and Southern California*, 211. Geological Society of America Memoir, pp. 263–316.

- Lackey, J.S., Valley, J.W., Saleeby, J.B., 2005. Supracrustal input to magmas in the deep crust of Sierra Nevada batholith: evidence from high- $\delta^{18}\text{O}$  zircon. *Earth Planet. Sci. Lett.* 235, 315–330.
- Klein, B.Z., Jagoutz, O., 2021. Construction of a trans-crustal magma system: Building the Bear Valley Intrusive Suite, southern Sierra Nevada, California. *Earth Planet. Sci. Lett.* 553, 116624.
- Klein, B.Z., Jagoutz, O., Ramezani, J., 2021. High-precision geochronology requires that ultrafast mantle-derived magmatic fluxes built the transcrustal Bear Valley Intrusive Suite, Sierra Nevada, California, USA. *Geology* 49, 106–110.
- Lackey, J.S., Valley, J.W., Chen, J.H., Stockli, D.F., 2008. Dynamic magma systems, crustal recycling, and alteration in the Central Sierra Nevada batholith: The oxygen isotope record. *J. Petrol.* 49, 1397–1426.
- Lallemand, S., Heuret, A., Faccenna, C., Funicello, F., 2008. Subduction dynamics as revealed by trench migration. *Tectonics* 27 (TC3014).
- Lambart, S., Laporte, D., Provost, A., Schiano, P., 2012. Fate of pyroxenite-derived melts in the peridotitic mantle: thermodynamic and experimental constraints. *J. Petrol.* 53, 451–476.
- Lambart, S., Baker, M.B., Stolper, E.M., 2016. The role of pyroxenite in basalt genesis: Melt-PX, a melting parameterization for mantle pyroxenites between 0.9 and 5 GPa. *J. Geophys. Res. Solid Earth* 121, 5708–5735.
- Lara, M., Dasgupta, R., 2020. Partial melting of a depleted peridotite metasomatized by a MORB-derived hydrous silicate melt—Implications for subduction zone magmatism. *Geochimica et Cosmochimica Acta* 290, 137–161.
- Lee, C.T.A., 2005. Trace element evidence for hydrous metasomatism at the base of the north American lithosphere and possible association with Laramide low-angle subduction. *J. Geol.* 113, 673–685.
- Lee, C.T.A., Cheng, X., Horodyskyj, U., 2006. The development and refinement of continental arcs by primary basaltic magmatism, garnet pyroxenite accumulation, basaltic recharge and delamination: insights from the Sierra Nevada, California. *Contrib. Mineral. Petrol.* 151, 222–242.
- Lee, C., King, S.D., 2011. Dynamic buckling of subducting slabs reconciles geological and geophysical observations. *Earth Planet. Sci. Lett.* 312, 360–370.
- Lee, C.T.A., Lackey, J.S., 2015. Global continental arc flare-ups and their relation to long-term greenhouse conditions. *Elements* 11, 125–130.
- Li, Z.X., Li, X.H., Chung, S.L., Lo, C.H., Xu, X., Li, W.X., 2012. Magmatic switch-on and switch-off along the South China continental margin since the Permian: transition from an Andean-type to a Western Pacific-type plate boundary. *Tectonophysics* 532, 271–290.
- Licht, A., Win, Z., Westerweel, J., Cogné, N., Morley, C.K., Chantraprasert, S., Poblete, F., Ugrai, T., Nelson, B., Aung, D.W., Dupont-Nivet, G., 2020. Magmatic history of Central Myanmar and implications for the evolution of the Burma Terrane. *Gondwana Res.* 87, 303–319.
- Linn, A.M., DePaolo, D.J., Ingersoll, R.V., 1992. Nd-Sr isotopic, geochemical, and petrographic stratigraphy and paleotectonic analysis: Mesozoic Great Valley forearc sedimentary rocks of California. *Geol. Soc. Am. Bull.* 104, 1264–1279.
- Lipman, P.W., 1992. Magmatism in the Cordilleran United States; progress and problems. In: Burchfiel, B.C., Lipman, P.W., Zoback, M.L. (Eds.), *The Cordilleran Orogen: Continents of the U.S. The Geology of North America*. Geological Society of America, Boulder, CO, pp. 481–514.
- Lipman, P.W., Probst, H.J., Christiansen, R.L., 1971. Evolving subduction zones in the western United States, as interpreted from igneous rocks. *Science* 174, 821–825.
- Mallik, A., Nelson, J., Dasgupta, R., 2015. Partial melting of fertile peridotite fluxed by hydrous rhyolitic melt at 2–3 GPa: implications for mantle wedge hybridization by sediment melt and generation of ultrapotassic magmas in convergent margins. *Contrib. Mineral. Petrol.* 169 (48).
- Mallik, A., Dasgupta, R., Tsuno, K., Nelson, J., 2016. Effects of water, depth and temperature on partial melting of mantle-wedge fluxed by hydrous sediment-melt in subduction zones. *Geochim. Cosmochim. Acta* 195, 226–243.
- Manea, V.C., Leeman, W.P., Gerya, T., Manea, M., Zhu, G., 2014. Subduction of fracture zones controls mantle melting and geochemical signature above slabs. *Nat. Commun.* 5, 1–10.
- Manga, M., Hornbach, M.J., Le Friant, A., Ishizuka, O., Stroncik, N., Adachi, T., Aljehdali, M., Boudon, G., Breikreuz, C., Fraass, A., Fujinawa, A., 2012. Heat flow in the Lesser Antilles island arc and adjacent back arc Grenada basin. *Geochem. Geophys. Geosyst.* 13 (8).
- Martinez-Ardila, A.M., Paterson, S.R., Memeti, V., Parada, M.A., Molina, P.G., 2019a. Mantle driven cretaceous flare-ups in Cordilleran arcs. *Lithos* 326, 19–27.
- Martinez-Ardila, A.M., Clausen, B.L., Memeti, V., Paterson, S.R., 2019b. Source contamination, crustal assimilation, and magmatic recycling during three flare-up events in the Cretaceous Peruvian Coastal Batholith: An example from the Ica-Pisco plutons. *J. S. Am. Earth Sci.* 95, 102300.
- Martinod, J., Husson, L., Roperch, P., Guillaume, B., Espurt, N., 2010. Horizontal subduction zones, convergence velocity and the building of the Andes. *Earth Planet. Sci. Lett.* 299, 299–309.
- McKenzie, N.R., Horton, B.K., Loomis, S.E., Stockli, D.F., Planavsky, N.J., Lee, C.T.A., 2016. Continental arc volcanism as the principal driver of icehouse-greenhouse variability. *Science* 352, 444–447.
- Milan, L.A., Daczko, N.R., Clarke, G.L., 2017. Cordillera Zealandia: a Mesozoic arc flare-up on the palaeo-Pacific Gondwana Margin. *Sci. Rep.* 7 (261).
- Mitchell, A.L., Grove, T.L., 2015. Melting the hydrous, subarc mantle: the origin of primitive andesites. *Contrib. Mineral. Petrol.* 170, 1–23.
- Moghadam, H.S., Li, X.H., Santos, J.F., Stern, R.J., Griffin, W.L., Ghorbani, G., Sarebani, N., 2017. Neoproterozoic magmatic flare-up along the N. margin of Gondwana: the Taknar complex, NE Iran. *Earth Planet. Sci. Lett.* 474, 83–96.
- Molnar, P., England, P., Martinod, J., 1993. Mantle dynamics, uplift of the Tibetan Plateau, and the Indian monsoon. *Rev. Geophys.* 31, 357–396.
- Müntener, O., Kelemen, P.B., Grove, T.L., 2001. The role of  $\text{H}_2\text{O}$  during crystallization of primitive arc magmas under uppermost mantle conditions and genesis of igneous pyroxenites: an experimental study. *Contrib. Mineral. Petrol.* 141, 643–658.
- Nelson, B.K., 1995. Fluid flow in subduction zones: evidence from Nd- and Sr-isotope variations in metabasalts of the Franciscan complex, California. *Contrib. Mineral. Petrol.* 119, 247–262.
- Newton, R.C., Manning, C.E., 2010. Role of saline fluids in deep-crustal and upper-mantle metasomatism: insights from experimental studies. *Geofluids* 10, 58–72.
- Nikolaeva, K., Gerya, T.V., Connolly, J.A., 2008. Numerical modelling of crustal growth in intraoceanic volcanic arcs. *Phys. Earth Planet. Inter.* 171, 336–356.
- Niu, Y., 2021. Lithosphere thickness controls the extent of mantle melting, depth of melt extraction and basalt compositions in all tectonic settings on Earth—A review and new perspectives. *Earth Sci. Rev.* 217, 103614.
- Noble, D.C., 1972. Some observations on the Cenozoic volcano-tectonic evolution of the Great Basin, western United States. *Earth Planet. Sci. Lett.* 17, 142–150.
- Oncken, O., Hindle, D., Kley, J., Elger, K., Victor, P., Schemmann, K., 2006. Deformation of the central Andean upper plate system—Facts, fiction, and constraints for plateau models. In: Oncken, O., Chong, G., Franz, G., Giese, P., Götze, H.J., Ramos, V.A., Strecker, M.R., Wigger, P. (Eds.), *The Andes*. Springer, Berlin, Heidelberg, pp. 3–27.
- O'Reilly, S.Y., Griffin, W.L., 2013. Mantle metasomatism. In: Harlov, D.E., Austrheim, H. (Eds.), *Metasomatism and the Chemical Transformation of Rock*. Berlin. Springer, Heidelberg, pp. 471–533.
- Otamendi, J.E., Ducea, M.N., Bergantz, G.W., 2012. Geological, petrological and geochemical evidence for progressive construction of an arc crustal section, Sierra de Valle Fertil, Famatinian Arc, Argentina. *J. Petrol.* 53, 761–800.
- Otamendi, J.E., Ducea, M.N., Cristofolini, E.A., Tibaldi, A.M., Camilletti, G.C., Bergantz, G.W., 2017. U-Pb ages and Hf isotope compositions of zircons in plutonic rocks from the central Famatinian arc, Argentina. *J. S. Am. Earth Sci.* 76, 412–426.
- Otamendi, J.E., Cristofolini, E.A., Morosini, A., Armas, P., Tibaldi, A.M., Camilletti, G.C., 2020. The geodynamic history of the Famatinian arc, Argentina: a record of exposed geology over the type section (latitudes 27°–33° south). *J. S. Am. Earth Sci.* 100 (102558).
- Paterson, S.R., Ducea, M.N., 2015. Arc magmatic tempos: gathering the evidence. *Elements* 11, 91–98.
- Paterson, S.R., Farris, D.W., 2008. Downward host rock transport and the formation of rim monoclines during the emplacement of Cordilleran batholiths: Transactions of the Royal Society of Edinburgh. *Earth Sci.* 97, 397–413.
- Paterson, S., Clausen, B., Memeti, V., Schwartz, J.J., 2017a. Arc magmatism, tectonism, and tempos in Mesozoic arc crustal sections of the Peninsular and Transverse Ranges, southern California, USA. In: *Field Excursions in Southern California: Field Guides to the 2016 GSA Cordilleran Section Meeting*, 45. Geological Society of America, p. 81.
- Paterson, S.R., Clausen, B., Memeti, V., Schwartz, J.J., 2017b. Arc magmatism, tectonism, and tempos in Mesozoic arc crustal sections of the Peninsular and Transverse Ranges, southern California, USA. In: Kraatz, B., Lackey, J.S., Fryxell, J.E. (Eds.), *Field Excursions in Southern California: Field Guides to the 2016 GSA Cordilleran Section Meeting*, 45. Geological Society of America Field Guide, pp. 81–196.
- Pepper, M., Gehrels, G., Pullen, A., Ibanez-Mejia, M., Ward, K.M., Kapp, P., 2016. Magmatic history and crustal genesis of western South America: constraints from U-Pb ages and Hf isotopes of detrital zircons in modern rivers. *Geosphere* 12, 1532–1555.
- Peslier, A.H., Francis, D., Ludden, J., 2002. The lithospheric mantle beneath continental margins: melting and melt-rock reaction in Canadian Cordillera xenoliths. *J. Petrol.* 43, 2013–2047.
- Petford, N., 2003. Rheology of granitic magmas during ascent and emplacement. *Ann. Rev. Earth Planet. Sci.* 31, 399–427.
- Petford, N., Gallagher, K., 2001. Partial melting of mafic (amphibolitic) lower crust by periodic influx of basaltic magma. *Earth Planet. Sci. Lett.* 193, 483–499.
- Petrelli, M., Zellmer, G.F., 2020. Rates and timescales of magma transfer, storage, emplacement, and eruption. In: *Vetere, F. (Ed.), Dynamic Magma Evolution*. American Geophysical Union Geophysical Monograph, pp. 1–41.
- Pickett, D.A., Saleeby, J.B., 1994. Nd, Sr, and Pb isotopic characteristics of Cretaceous intrusive rocks from deep levels of the Sierra Nevada batholith, Tehachapi Mountains, California. *Contrib. Mineral. Petrol.* 118, 198–215.
- Plank, T., Langmuir, C.H., 1988. An evaluation of the global variations in the major element chemistry of arc basalts. *Earth Planet. Sci. Lett.* 90, 349–370.
- Platt, J.P., 1986. Dynamics of orogenic wedges and the uplift of high-pressure metamorphic rocks. *Geol. Soc. Am. Bull.* 97, 1037–1053.
- Portner, D.E., Rodríguez, E.E., Beck, S., Zandt, G., Scire, A., Rocha, M.P., Bianchi, M.B., Ruiz, M., França, G.S., Condori, C., Alvarado, P., 2020. Detailed structure of the subducted Nazca Slab into the lower mantle derived from continent-scale teleseismic P wave tomography. *J. Geophys. Res. Solid Earth* 125 (e2019JB017884).
- Portnyagin, M., Hoernle, K., Plechov, P., Mironov, N., Khubunaya, S., 2007. Constraints on mantle melting and composition and nature of slab components in volcanic arcs from volatiles ( $\text{H}_2\text{O}$ , S, Cl, F) and trace elements in melt inclusions from the Kamchatka Arc. *Earth Planet. Sci. Lett.* 255, 53–69.
- Profeta, L., Ducea, M.N., Chapman, J.B., Paterson, S.R., Gonzales, S.M.H., Kirsch, M., Petrescu, L., DeCelles, P.G., 2015. Quantifying crustal thickness over time in magmatic arcs. *Sci. Rep.* 5, 1–7.
- Ramos, V.A., 2009. Anatomy and global context of the Andes: Main geologic features and the Andean orogenic cycle. In: Kay, S.M. (Ed.), *Backbone of the Americas: Shallow Subduction, Plateau Uplift, and Ridge and Terrane Collision*, 204. Geological Society of America Memoir, pp. 31–65.
- Ramos, V.A., Cristallini, E.O., Pérez, D.J., 2002. The Pampean flat-slab of the Central Andes. *J. S. Am. Earth Sci.* 15 (1), 59–78.

- Ratschbacher, B.C., Paterson, S.R., Fischer, T.P., 2019. Spatial and depth-dependent variations in magma volume addition and addition rates to continental arcs: application to global CO<sub>2</sub> fluxes since 750 Ma. *Geochemistry, Geophysics, Geosystems*, v. 20, 2997–3018.
- Reymer, A., Schubert, G., 1984. Phanerozoic addition rates to the continental crust and crustal growth. *Tectonics* 3, 63–77.
- Ribe, N.M., Stutzmann, E., Ren, Y., Van der Hilst, R., 2007. Buckling instabilities of subducted lithosphere beneath the transition zone. *Earth Planet. Sci. Lett.* 254, 173–179.
- Ridolfi, F., Renzulli, A., Puerini, M., 2010. Stability and chemical equilibrium of amphibole in calc-alkaline magmas: an overview, new thermobarometric formulations and application to subduction-related volcanoes. *Contrib. Mineral. Petrol.* 160, 45–66.
- Riel, N., Bouilhol, P., van Hunen, J., Cornet, J., Magni, V., Grigороva, V., Velic, M., 2019. Interaction between mantle-derived magma and lower arc crust: quantitative reactive melt flow modelling using Stxk. *Geol. Soc. Lond., Spec. Publ.* 478, 65–87.
- Riley, T.R., Burton-Johnson, A., Flowerdew, M.J., Whitehouse, M.J., 2018. Episodicity within a mid-Cretaceous magmatic flare-up in West Antarctica: U-Pb ages of the Lassiter Coast intrusive suite, Antarctic Peninsula, and correlations along the Gondwana margin. *Geol. Soc. Am. Bull.* 130, 1177–1196.
- Rodríguez, G., Arango, M.I., Zapata, G., Bermúdez, J.G., 2018. Petrotectonic characteristics, geochemistry, and U-Pb geochronology of Jurassic plutons in the Upper Magdalena Valley-Colombia: implications on the evolution of magmatic arcs in the NW Andes. *J. S. Am. Earth Sci.* 81, 10–30.
- Rodríguez, E.E., Portner, D.E., Beck, S.L., Rocha, M.P., Bianchi, M.B., Assumpção, M., Ruiz, M., Alvarado, P., Condori, C., Lynner, C., 2021. Mantle dynamics of the Andean Subduction Zone from continent-scale teleseismic S-wave tomography. *Geophys. J. Int.* 224, 1553–1571.
- Rosenbaum, G., 2018. The Tasmanides: phanerozoic tectonic evolution of eastern Australia. *Annu. Rev. Earth Planet. Sci.* 46, 291–325.
- Rosenberg, C.L., Handy, M.R., 2005. Experimental deformation of partially melted granite revisited: implications for the continental crust. *J. Metamorph. Geol.* 23, 19–28.
- Ruscitto, D.M., Wallace, P.J., Cooper, L.B., Plank, T., 2012. Global variations in H<sub>2</sub>O/Ce: 2. Relationships to arc magma geochemistry and volatile fluxes. *Geochem. Geophys. Geosyst.* 13 (3).
- Rushmer, T., Miller, S.A., 2006. Melt migration in the continental crust and generation of lower crustal permeability: inferences from modeling and experimental studies. In: Brown, M., Rushmer, T. (Eds.), *Evolution and differentiation of the continental crust*. Cambridge University Press, pp. 430–454.
- Saleeby, J.B., 1990. Progress in tectonic and petrogenetic studies in an exposed cross-section of young (~100 Ma) continental crust, southern Sierra Nevada, California. In: Salisbury, M.H., Fountain, D.M. (Eds.), *Exposed Cross-Sections of the Continental Crust*. Springer, Dordrecht, pp. 137–158.
- Saleeby, J., Ducea, M., Clemens-Knott, D., 2003. Production and loss of high-density batholithic root, southern Sierra Nevada, California. *Tectonics* 22.
- Sawyer, E.W., 1994. Melt segregation in the continental crust. *Geology* 22, 1019–1022.
- Schellart, W.P., 2008. Subduction zone trench migration: slab driven or overriding-plate-driven? *Phys. Earth Planet. Inter.* 170, 73–88.
- Schellart, W.P., 2017. Andean mountain building and magmatic arc migration driven by subduction-induced whole mantle flow. *Nat. Commun.* 8, 1–13.
- Schleiffarth, W.K., Darin, M.H., Reid, M.R., Umhoefer, P.J., 2018. Dynamics of episodic late Cretaceous–Cenozoic magmatism across Central to Eastern Anatolia: New insights from an extensive geochronology compilation. *Geosphere* 14, 1990–2008.
- Schmidt, M.W., Poli, S., 1998. Experimentally based water budgets for dehydrating slabs and consequences for arc magma generation. *Earth Planet. Sci. Lett.* 163, 361–379.
- Schütte, P., Chiaradia, M., Beate, B., 2010. Geodynamic controls on Tertiary arc magmatism in Ecuador: Constraints from U–Pb zircon geochronology of Oligocene–Miocene intrusions and regional age distribution trends. *Tectonophysics* 489, 159–176.
- Schwartz, J.J., Klepeis, K.A., Sadowski, J.F., Stowell, H.H., Tulloch, A.J., Coble, M.A., 2017. The tempo of continental arc construction in the Mesozoic Median Batholith, Fiordland, New Zealand. *Lithosphere* 9, 343–365.
- Schwartz, J.J., Andico, S., Turnbull, R., Klepeis, K.A., Tulloch, A.J., Kitajima, K., and Valley, J., in press. Stable and transient isotopic trends in the Crustal Evolution of Zealandia Cordillera. *Am. Mineral.*, doi:<https://doi.org/10.2138/am-2021-7626>.
- Sepidar, F., Mirnejad, H., Ma, C., Moghadam, H.S., 2018. Identification of Eocene–Oligocene magmatic pulses associated with flare-up in East Iran: timing and sources. *Gondwana Res.* 57, 141–156.
- Shea, E.K., Miller, J.S., Miller, R.B., Chan, C.F., Kent, A.J., Hanchar, J.M., Dustin, K., Elkins, S., 2018. Time scale for the development of thickened crust in the Cretaceous North Cascades magmatic arc, Washington, and relationship to Cretaceous flare-up magmatism. *Lithosphere* 10, 708–722.
- Sillitoe, R.H., 2018. Why no porphyry copper deposits in Japan and South Korea? *Resour. Geol.* 68, 107–125.
- Silver, L.T., Chappell, B.W., 1988. The Peninsular Ranges Batholith: an insight into the evolution of the Cordilleran batholiths of southwestern North America. *Earth Environ. Sci. Trans. Royal Soc. Edinburgh* 79, 105–121.
- Smith, P.M., Asimow, P.D., 2005. *Adiabat\_1ph*: A new public front-end to the MELTS, pMELTS, and pHMELTS models. *Geochem. Geophys. Geosyst.* 6, 1–8.
- Solano, J.M.S., Jackson, M.D., Sparks, R.S.J., Blundy, J.D., Annen, C., 2012. Melt segregation in deep crustal hot zones: a mechanism for chemical differentiation, crustal assimilation and the formation of evolved magmas. *J. Petrol.* 53, 1999–2026.
- Stegman, D.R., Schellart, W.P., Freeman, J., 2010. Competing influences of plate width and far-field boundary conditions on trench migration and morphology of subducted slabs in the upper mantle. *Tectonophysics* 483, 46–57.
- Stern, C.R., 2011. Subduction erosion: rates, mechanisms, and its role in arc magmatism and the evolution of the continental crust and mantle. *Gondwana Res.* 20, 284–308.
- Straub, S.M., Gómez-Tuena, A., Vannucchi, P., 2020. Subduction erosion and arc volcanism. *Nat. Rev. Earth Environ.* 1, 574–589.
- Sundell, K., Saylor, J.E., Pecha, M., 2019. Provenance and recycling of detrital zircons from Cenozoic Altiplano strata and the crustal evolution of western South America from combined U–Pb and Lu–Hf isotopic analysis. In: Horton, B.K., Folguera, A. (Eds.), *Andean Tectonics*. Elsevier, pp. 363–397.
- Taylor Jr., H.P., 1978. Oxygen and hydrogen isotope studies of plutonic granitic rocks. *Earth Planet. Sci. Lett.* 38, 177–210.
- Torsvik, T.H., Müller, R.D., Van der Voo, R., Steinberger, B., Gaina, C., 2008. Global plate motion frames: toward a unified model. *Rev. Geophys.* 46, RG3004.
- Torsvik, T.H., Steinberger, B., Shephard, G.E., Doubrovine, P.V., Gaina, C., Domeier, M., Conrad, C.P., Sager, W.W., 2019. Pacific–Panthalassic reconstructions: overview, errata and the way forward. *Geochem. Geophys. Geosyst.* 20, 3659–3689.
- Triantafyllou, A., Berger, J., Baele, J.M., Mattielli, N., Ducea, M.N., Sterckx, S., Samson, S., Hodel, F., Ennih, N., 2020. Episodic magmatism during the growth of a Neoproterozoic oceanic arc (Anti-Atlas, Morocco). *Precambrian Res.* 339 (105610).
- Tulloch, A.J., Kimbrough, D.L., 2003. Paired plutonic belts in convergent margins and the development of high Sr/Y magmatism: the Peninsular Ranges Batholith of California and the Median Batholith of New Zealand. In: Johnson, S.E., Paterson, S.E., Fletcher, J.M., Girty, G.H., Kimbrough, D.L., Martin-Barajas, A. (Eds.), *The Tectonic Evolution of Northwestern Mexico and the Southwestern USA*, 374. Geological Society of America Special Paper, pp. 275–295.
- Turner, S.J., Langmuir, C.H., 2015a. The global chemical systematics of arc front stratovolcanoes: evaluating the role of crustal processes. *Earth Planet. Sci. Lett.* 422, 182–193.
- Turner, S.J., Langmuir, C.H., 2015b. What processes control the chemical compositions of arc front stratovolcanoes? *Geochem. Geophys. Geosyst.* 16 (6), 1865–1893.
- Turner, S., Arnaud, N., Liu, J., Rogers, N., Hawkesworth, C., Harris, N., Kelley, S.V., Van Calsteren, P., Deng, W., 1996. Post-collision, shoshonitic volcanism on the Tibetan Plateau: implications for convective thinning of the lithosphere and the source of ocean island basalts. *J. Petrol.* 37, 45–71.
- Turner, S., Hawkesworth, C., Rogers, N., Bartlett, J., Worthington, T., Hergt, J., Pearce, J., Smith, I., 1997. <sup>238</sup>U–<sup>230</sup>Th disequilibria, magma petrogenesis, and flux rates beneath the depleted Tonga–Kermadec island arc. *Geochim. Cosmochim. Acta* 61, 4855–4884.
- Ulmer, P., 2001. Partial melting in the mantle wedge—the role of H<sub>2</sub>O in the genesis of mantle-derived ‘arc-related’ magmas. *Phys. Earth Planet. Inter.* 127, 215–232.
- Valley, J.W., 2003. Oxygen isotopes in zircon. *Rev. Mineral. Geochem.* 53, 343–385.
- van der Molen, I., Paterson, M.S., 1979. Experimental deformation of partially-melted granite. *Contrib. Mineral. Petrol.* 70, 299–318.
- van Keken, P.E., Hacker, B.R., Syracuse, E.M., Abers, G.A., 2011. Subduction factory: 4. Depth-dependent flux of H<sub>2</sub>O from subducting slabs worldwide. *J. Geophys. Res. Solid Earth* 116 (B1).
- Vervoort, J.D., Patchett, P.J., Blichert-Toft, J., Albarède, F., 1999. Relationships between Lu–Hf and Sm–Nd isotopic systems in the global sedimentary system. *Earth Planet. Sci. Lett.* 168, 79–99.
- Vogt, K., Gerya, T.V., Castro, A., 2012. Crustal growth at active continental margins: numerical modeling. *Phys. Earth Planet. Inter.* 192, 1–20.
- Wada, I., Behn, M.D., 2015. Focusing of upward fluid migration beneath volcanic arcs: effect of mineral grain size variation in the mantle wedge. *Geochem. Geophys. Geosyst.* 16, 3905–3923.
- Walker Jr., B.A., Bergantz, G.W., Otamendi, J.E., Ducea, M.N., Cristofolini, E.A., 2015. A MASH zone revealed: the mafic complex of the Sierra Valle Fértil. *J. Petrol.* 56, 1863–1896.
- Wells, M.L., Hoisch, T.D., 2008. The role of mantle delamination in widespread Late Cretaceous extension and magmatism in the Cordilleran orogen, western United States. *Geol. Soc. Am. Bull.* 120, 515–530.
- Wetmore, P.H., Ducea, M.N., 2011. Geochemical evidence of a near-surface history for source rocks of the central Coast Mountains Batholith, British Columbia. *Int. Geol. Rev.* 53, 230–260.
- Whattam, S.A., Cho, M., Smith, I.E., 2011. Magmatic peridotites and pyroxenites, Andong Ultramafic Complex, Korea: geochemical evidence for supra-subduction zone formation and extensive melt–rock interaction. *Lithos* 127, 599–618.
- Yang, Q.Y., Santosh, M., 2015. Early Cretaceous magma flare-up and its implications on gold mineralization in the Jiaodong Peninsula, China. *Ore Geol. Rev.* 65, 626–642.
- Yang, J., Cao, W., Gordon, S.M., Chu, X., 2020. Does underthrusting crust feed magmatic flare-ups in continental arcs? *Geochem. Geophys. Geosyst.* 21 (e2020GC009152).
- Yoder, J.A., et al., 2020. A Vision for NSF Earth Sciences 2020–2030: Earth in Time: National Academies of Sciences, Engineering, and Medicine. The National Academies Press, Washington, D.C., p. 144.
- Zellmer, G.F., 2008. Some first-order observations on magma transfer from mantle wedge to upper crust at volcanic arcs. *Geol. Soc. Lond., Spec. Publ.* 304, 15–31.
- Zhang, L.L., Zhu, D.C., Wang, Q., Zhao, Z.D., Liu, D., Xie, J.C., 2019a. Late Cretaceous volcanic rocks in the Sangri area, southern Lhasa Terrane, Tibet: Evidence for oceanic ridge subduction. *Lithos* 326, 144–157.
- Zhang, X., Chung, S.L., Lai, Y.M., Ghani, A.A., Murtadha, S., Lee, H.Y., Hsu, C.C., 2019b. A 6000-km-long Neo-Tethyan arc system with coherent magmatic flare-ups and lulls in South Asia. *Geology* 47, 573–576.

Zhu, G., Gerya, T.V., Tackley, P.J., Kissling, E., 2013. Four-dimensional numerical modeling of crustal growth at active continental margins. *J. Geophys. Res. Solid Earth* 118, 4682–4698.

Zhu, D.C., Mo, X.X., Niu, Y., Zhao, Z.D., Wang, L.Q., Liu, Y.S., Wu, F.Y., 2009. Geochemical investigation of Early Cretaceous igneous rocks along an east–west traverse throughout the central Lhasa Terrane Tibet. *Chem. Geol.* 268, 298–312.

Zhu, D.C., Wang, Q., Chung, S.L., Cawood, P.A., Zhao, Z.D., 2019. Gangdese magmatism in southern Tibet and India–Asia convergence since 120 Ma. In: Treloar, P.J., Searle, M.J. (Eds.), *Himalayan Tectonics: A Modern Synthesis*, 483. Geological Society, London, Special Publication, pp. 583–604.